A Combined Method for Establishing Keratinocyte Cultures from Cervical Biopsy Specimens and Creating Patient-Derived 3-Dimensional Organotypic Raft Cultures

A thesis presented to

The Faulty of Graduate Studies

of

Lakehead University

by

PETER L. VILLA

In partial fulfillment of requirements

for the degree of

Master of Science

in

Biology

Abstract

High-risk types of human papillomavirus (HPV) are responsible for nearly all instances of cervical cancer, and a significant proportion of head and neck cancers. Studying HPV in the laboratory requires the cultivation of host keratinocytes to facilitate the viral lifecycle. In addition, HPV will not completely undergo its lifecycle in monolayer cell culture, but requires the differentiation process of keratinocytes. This can be accomplished by employing organotypic raft cultures, which simulates full-thickness skin *in vitro*. Though this method can reproduce the viral lifecycle, there are still numerous hurdles when modelling disease. In the first phase of this study, we utilize published methods to culture cervical keratinocytes from 25 different cervical lesion biopsies, establishing cultures from 8 (~32%). Biopsy specimens were digested with collagenase I and grown in keratinocyte growth medium (KGM) containing 5% fetal bovine serum for 4 days, after which, cultures were switched to serum-free KGM to avoid fibroblast overgrowth. The median *in vitro* lifespan of cultures was 4 weeks, which typically yielded less than a confluent T-75 of cells. In the second phase of this study, the media was switched from KGM to EpiLife, which has more organic components, and contains insulin-like growth factor I in place of insulin, which has more mitogenic potential and increases keratinocyte lifespan *in vitro*. Biopsies were processed under the same conditions, and after removing the media containing 5% serum, the Rho-associated kinase (ROCK) inhibitor Y-27632 was added to EpiLife media to further increase culture lifespan. Cultures were established from 6 of 14 (~42%) newly acquired biopsies, 4 of which survived for several passages (range 2-7) across T-75 flasks (flasks seeded at 10% confluence and passaged when >80% confluent). The improved culture conditions effectively halved the doubling time, but maintained

approximately the same culture lifespan (median 4.5 weeks). Organotypic raft cultures were prepared using 5 different patient samples; most had differentiated at the time of 3D culturing, while others yielded only a few cell layers upon cross sectioning and H&E staining. Future work will improve upon our culture media formulations to facilitate stratification of raft cultures, and potentially improve culture lifespan further.

Lay Summary

Human papillomavirus (HPV) is a virus that infects cells of the skin and mucosa. HPV is the infectious agent responsible for warts, and notably, HPV is also responsible for nearly all instances of cervical cancer. Studying HPV in the laboratory requires the culture of its host cells – called keratinocytes. Human keratinocytes grown in the laboratory are typically acquired from neonatal foreskins. This tissue is readily accessible and would otherwise be discarded, making it both practical and ethical means of acquiring keratinocytes. Though the virus can replicate within these cells under the appropriate conditions, cervical keratinocytes would be a more accurate model for studying HPV-mediated cervical cancer. In this study, we expanded upon published methods to culture keratinocytes from cervical biopsy specimens. In the first phase of this study we established 8 cultures from 25 biopsy specimens, with the median culture actively growing for 4 weeks. Most of these cultures did not proliferate enough for further experimentation. Therefore, the second phase of this study sought to increase culture lifespan. We replaced our media with EpiLife, a formulation which is rated for more than twice as many population doublings. We also added the protein kinase inhibitor Y-27632 which prevents keratinocyte differentiation, thereby increasing their lifespan. We established cultures from 6 of 14 newly enrolled patients. Median survival was modestly increased to 4.5 weeks, but the doubling time was nearly halved. Most of these cultures proliferated enough to be utilized in further experimentation. We attempted to reconstruct these cells into 3-dimensional cultures *in vitro*, to simulate patient lesions – albeit with limited success. Future work will improve upon our 3D culture methods with aims at modelling patient lesions and testing new therapeutics.

Dedication

To those who pursue practicality over prestige

Acknowledgements

Professional

First and foremost, I would like to thank Dr. Ingeborg Zehbe for providing me with the great opportunity to pursue graduate studies under her supervision, to allow me to pursue much of my work at my own devices, and to be part of her extensive research network and collaborations. Next, I'd like to thank Dr. Nicholas Escott for collaborating as a co-investigator on this research project, as well as Bonnie Kozak, Maita Mauro, and Brenda Kulifaj for consenting patients and contributing to this study. Without your participation (also provided in gratis), the clinical components of this work would not have been possible. Additional thanks to Dr. Alberto Severini for providing his expert HPV-typing services in kind, and Marisa Kubinec for facilitating much of our required pathology services.

I'd like to thank my committee members: Dr. Simon Lees and Dr. Neelam Khaper, your patience and understanding is greatly appreciated; and my external examiner Dr. Robert Lafrenie, who has also been an excellent source of knowledge during my early research career.

I'd also like to thank the Clinical Research Services Department, and the Research Ethics Boards (at both Lakehead University and the Thunder Bay Regional Health Sciences Centre) for facilitating the documentation, training, and approval of this project.

Lastly, I'd like to thank the members of the laboratory: Robert Jackson, Melissa Togtema, Jessica Grochowski, and Vanessa Masters. Without your contributions and collaboration, I would never be able to navigate my weekly tasks.

Personal

First, I'd like to thank my friends and family, who have been a source of both financial and emotional support over the past two years. Next, I'd like to thank my roommate Mirjana Vrabanac for providing me with a place to live once moving to Thunder Bay, and Lauren Hayhurst for maintaining my sanity while here. I'd like to thank Shannon Maki for the nice conversations, Tanya Niederer for the humouring input, and Carmen Dore for laughing at all my jokes.

I'd also like to thank the ladies from health records: Joanne Waddington, for your down-to-earth conversations, and Christine Deschamps, for our nice little coffee dates. Sporadic weekly small talks are an occurrence that I am going to miss.

Table of Contents

List of Tables

List of Figures

List of Abbreviations

bp   Base-pair

cDNA   Complementary DNA

CIN   Cervical Intraepithelial Neoplasia

CO2   Carbon Dioxide

Ct   Cycle threshold

DAPI   4',6-diamidino-2-phenylindole

dH2O   Distilled Water

DMEM   Dulbecco's Modified Eagle Medium

DMSO   Dimethyl Sulfoxide

DNA   Deoxyribonucleic Acid

dsDNA   Double Stranded Deoxyribonucleic Acid

DPBS   Dulbecco's Phosphate Buffered Saline

DsiRNA   Dicer-substrate siRNA

EBV   Epstein-Barr Virus

EDTA   Ethylenediaminetetraacetic Acid

EGF   Epidermal Growth Factor

FBS   Fetal Bovine Serum

HPRT1   Hypoxanthine Phosphoribosyltransferase 1

HPV   Human Papillomavirus

hTERT   Human Telomerase Reverse Transcriptase

IGF-I   Insulin-like Growth Factor I

IHC   Immunohistochemistry

KGM	Keratinocyte Growth Medium
MAPK	Mitogen-activated Protein Kinase
MCM2	Minichromosome Maintenance Protein 2
mRNA	Messenger RNA
NIKS	Normal or Near-diploid Immortal Keratinocytes
nt	Nucleotides
p53	Tumour Suppressor Protein 53
PCR	Polymerase Chain Reaction
pRB	Retinoblastoma Protein
RISC	RNA Induced Silencing Complex
RNA	Ribonucleic Acid
RQI	RNA Quality Indicator
RT-qPCR	Reverse Transcription, Real-Time PCR
SD	Standard Deviation
siRNA	Small-interfering RNA
TOP2A	Topoisomerase IIA

1. Introduction

1.1 Human papillomavirus literature review

1.1.1 General overview of human papillomavirus and disease

Human papillomavirus (HPV) is a double-stranded DNA virus that infects keratinocytes of the skin and mucosa (zur Hausen, 2002). To date, over 200 distinct types of HPV have been recognized (de Villiers, 2013; Papillomavirus Episteme <https://pave.niaid.nih.gov/#home>), which are broadly categorized as high- or low-risk types based on their ability to cause cancer. The most clinically significant high-risk type is HPV16, which accounts for approximately half of all HPV-related cervical and a significant portion of head and neck cancer cancers (Crow, 2012). Possessing a small circular genome of ~7900 base pairs, HPV16 has eight genes, some of which contain splice variants (Zheng and Baker, 2006). The most notable of these viral genes are the two oncogenes: E6 and E7. In HPV16, the E6 oncoprotein facilitates the degradation of the host tumour-suppressor p53, while also increasing telomerase expression; thereby inhibiting apoptosis and facilitating cellular immortalization. The E7 oncoprotein mediates degradation of pRB, promoting entry into the cell-cycle (Klingelhutz and Roman, 2012). Together, E6 and E7 promote cellular transformation and subsequent tumourigenesis.

1.1.2 HPV viral life cycle, histological changes, and cancer

The HPV virions infect basal keratinocytes through epidermal micro-abrasions (zur Hausen, 2002), where basal keratinocytes are the actively dividing cells in the epithelium. As early genes, E6 and E7 inhibit apoptosis and maintain cellular division, as stated

previously (**Figure 1A**). Early during infection, E1 and E2 maintain low-level viral genome replication, while E2 also modulates host and viral transcription (Frattini and Laimins, 1994; Wilson *et al.*, 2002). Later into the viral life cycle, E4 (Peh *et al.*, 2004) and E5 (Genther *et al.*, 2003) further promote viral genome amplification, and viral particles are assembled with the major- and minor-capsid proteins L1 and L2, respectively. Assembled HPV virions are then shed from the cornified layer.

HPV inhibits the differentiation of keratinocytes, which has numerous histological corollaries of both clinical and experimental significance. Physiological differentiation triggers keratin switching in the epithelial layer, Keratin 5 (K5) expression is high in the basal layer (Moll *et al.*, 1982); Keratin 10 (K10) and involucrin expression begins in the spinous layer and continues through to the cornified layer (Strudwick *et al.*, 2015; **Figure 1B**). Therefore, HPV infection will increase the spatial expression of K5 past the basal layer, and impede the expression of K10 and involucrin at the spinous layer. This abrogated differentiation is accompanied by the retention of cell nuclei beyond the basal layer. These biomarkers can be stained for via immunohistochemistry (IHC) in both patient biopsy specimens, and organotypic raft cultures growth *in vitro* (described below). Of clinical relevance however, there are other biomarkers of interest.
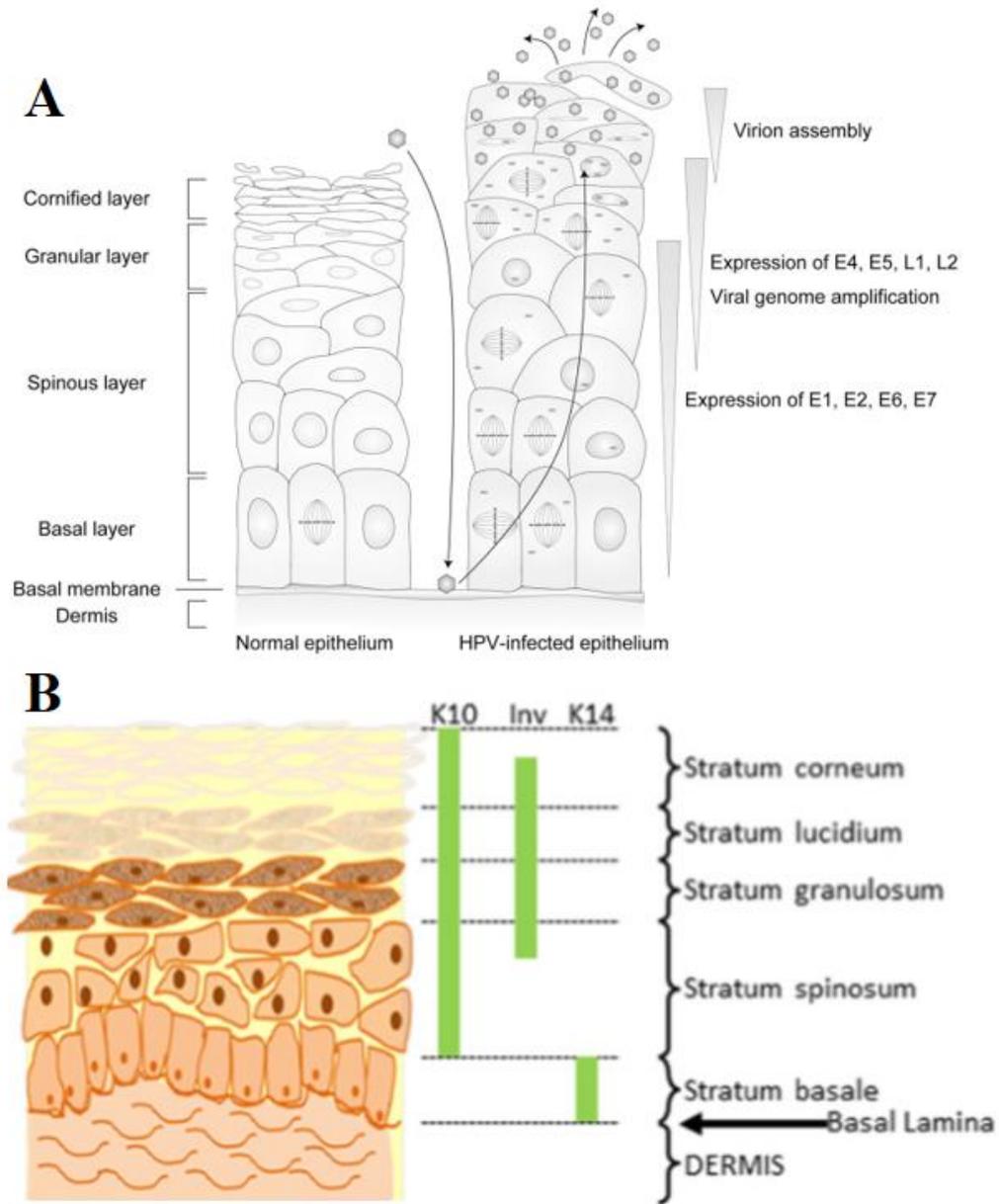
Figure 1. Spatial expression of HPV viral genes during infection of skin. HPV virions infect basal keratinocytes through micro-abrasions (**A**). The viral oncogenes E6 and E7 inhibit apoptosis and promote entry into the cell cycle, while E1 and E2 maintain low-level viral genome replication. The viral genes E4 and E5 promote viral genome amplification and assemble with the capsid proteins L1 and L2. Viral particles are released as cells slough off (modified from Kajitani et al., 2012). Spatial expression of biomarkers markers during epithelial differentiation (**B**; Strudwick et al., 2015).

Clinical biomarkers – those used to assess cervical lesion progression – are typically related to cell cycle regulation. The most commonly assessed is the cyclin-dependant kinase inhibitor p16^{INK4a}. Increased p16^{INK4a} expression is a consequence of E7-mediated disruption of pRB (Wentzensen *et al.*, 2007). Other tests exist to detect for aberrant S-phase induction, namely topoisomerase IIA (TOP2A) and minichromosome maintenance protein 2 (MCM2; Halloush *et al.*, 2008). Increases in p16^{INK4a}, TOP2A, or MCM2 indicates a lesion progressing to high-grade. These tests are generally combined with hemotoxylin and eosin (H&E) staining of patient biopsy sections to help evaluate the neoplastic lesion. **Figure 2** illustrates the infection process, low- to high- grade lesion progression, and finally invasive cancer. Of course, other prognostic markers relating to the virus itself are occasionally tested. HPV typing can determine if a patient is infected with a high-risk HPV type, as well elevated expression levels of the E6 and E7 oncogenes (Cattani *et al.*, 2009). Also, as integration of the viral episome into the host genome is present in the majority of cervical carcinomas, testing for integration status may also suggest a progressing cervical lesion (Peitsaro *et al.*, 2002).
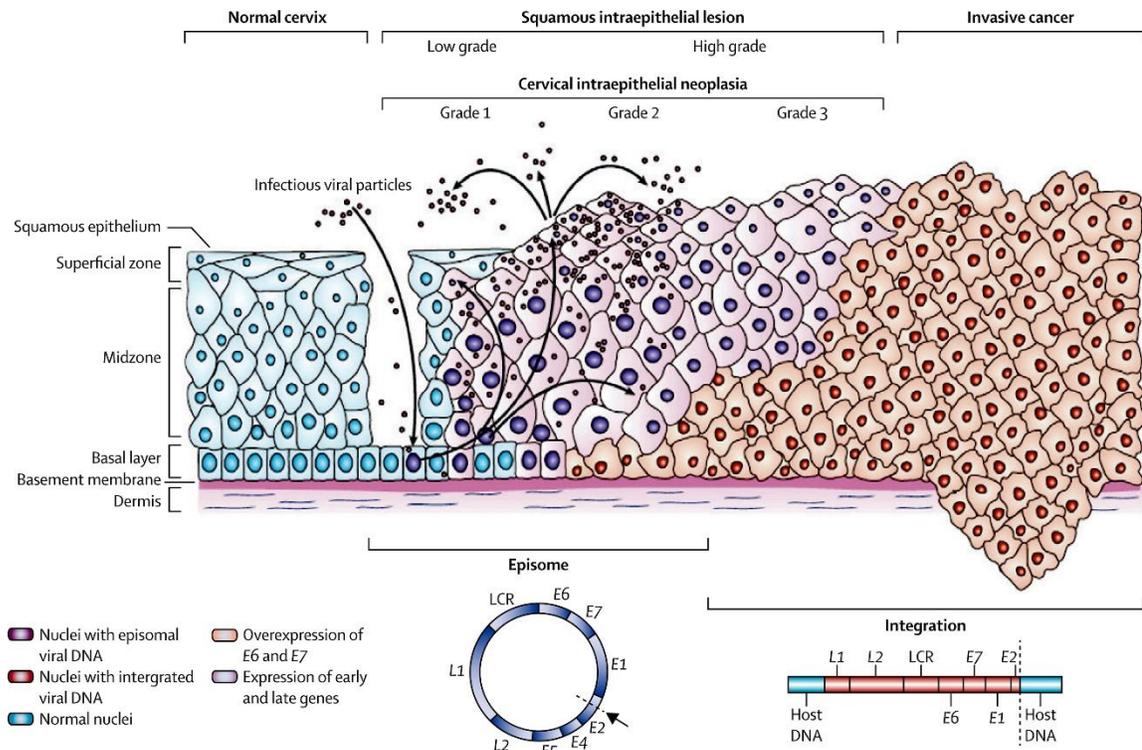
Figure 2. Cervical lesion progression towards cancer. HPV infects basal keratinocytes through a micro-abrasion. Infection prevents keratinocyte differentiation, causing cells to retain their nuclei for longer, producing viral particles. In most instances of HPV-mediated carcinogenesis, the viral genome integrates into the host genome. Overexpression of E6 and E7 promotes the progression of high-grade lesions towards invasive carcinoma (Woodman *et al.*, 2007).

1.1.3 Organotypic raft culture

Organotypic raft cultures are three-dimensional cultures which simulate full-thickness skin, created from monolayer cultures grown entirely *in vitro* (Bell *et al.*, 1981). Organotypic raft cultures can be constructed using primary cell lines, immortalized cell lines, or both. They consist of a simulated dermis containing fibroblast cells, and a keratinocyte monolayer seeded on top; grown at an air-liquid interface to facilitate epithelialization. Different methods utilize primary (Jackson *et al.*, 2014) or immortalized fibroblasts (Pickard *et al.*, 2015), in combination with primary or immortalized keratinocytes (Strudwick *et al.*, 2015), whereby mucosal keratinocytes can also be utilized

5

to model mucosal epithelium (Dongari-Bagtzoglou and Kashleva, 2006). Importantly, raft cultures can model normal and dysplastic epithelium (Blanton *et al*., 1991), and have also been employed to study numerous viruses besides HPVs, including poxviruses (Duraffour *et al*, 2007), Epstein-Barr virus (Dawson *et al.*, 1998), and herpes simplex virus (Hukkanen *et al.*, 1999). For HPV, the raft model is not only permissive to the differentiation-dependant viral life-cycle (Meyers *et al.*, 1992; Flores *et al.*, 1999), it has even been shown to reproduce epithelial invasion of the dermis when using E6/E7 transduced cell lines (Pickard *et al.*, 2015). In this respect, it may be possible to use raft cultures to model lesion progression and early invasion, using patient-derived cell lines. Raft cultures have additional uses when studying viral exanthems, as they maintain many pathogen-host interactions while bypassing the need for animal models. Indeed, organotypic raft cultures have been used to test antiviral drugs against herpes viruses (Andrei, 2005) and poxviruses (Duaffour *et al*., 2007), as well as topical treatments for head and neck squamous cell carcinoma (Eicher *et al.*, 1996). It would seem feasible then, to test new antiviral agents against HPV in organotypic raft cultures.

1.1.4 Establishment of cervical keratinocyte cell cultures

Primary neonatal foreskin keratinocytes are the most commonly utilized human keratinocyte in the laboratory. Foreskins are easy to acquire – both practically and ethically speaking – and a foreskin can yield many more cells over a biopsy. Ideally when studying cervical cancer, a researcher would obviously utilize cervical cells. There are two means to acquire primary cervical cells: 1) isolate and culture normal cervical keratinocytes from a healthy cervix, and introduce HPV experimentally; and 2) propagate cells derived from

naturally-infected cervical lesion biopsies. Unfortunately, there are numerous practical and ethical hurdles when establishing cultures of normal primary cervical keratinocytes. First and foremost, it is unethical to acquire apparently healthy cervical tissue by biopsying a patient, as this introduces unnecessary risks, especially as many patients are of reproductive age. Therefore, the ideal means of acquiring healthy cervical tissue is from a total hysterectomy, which completely removes the uterus, cervix, and ovaries. Acquiring cervical tissue from a total hysterectomy has many practical challenges however, and requires the direct collaboration of the obstetrician/gynecologist performing the procedure and the acting pathologist, which ensures the patient's standard-of-care without formalin-fixing the still-living tissue.

The most practical and ethical means of acquiring cervical cells is to take biopsy specimens from patient lesions, while the physician is already taking a sample for standard-of-care. Given that cervical cancer results from persistent HPV infections, this approach would seem ideal for modelling and studying progression of cervical lesions. There are however, numerous methodological hurdles to establishing an *in vitro* culture of keratinocytes from biopsy specimens. These issues can include – but are not limited to – microbial contamination, fibroblast contamination (Stanley, 2002), low cellular viability and/or yield, and limited culture lifespan (Schweinfurth and Meyers, 2006). Previous studies have demonstrated low colony forming efficiency (Bononi *et al.*, 2012), limited potential to passage cultures (Liu *et al*, 2013), and low adherence of viable cells (Liu *et al*, 2016). Even with established methods, cultures from HPV lesions may be established from less than one-third of biopsy specimens and possess a limited lifespan *in vitro* (Schweinfurth and Meyers, 2006). Currently, there is no literature on generating

organotypic rafts from patient-derived, naturally-infected cervical keratinocytes.

1.1.5 Surveillance and intervention of cervical lesions

The vast majority of cervical HPV infections clear up naturally within three years (Ho *et al.*, 1998). A patient's standard-of-care is to have their cervical lesion monitored through Papanicolaou tests and colposcopy exams, rather than to surgically intervene at the first sight of a lesion. In Canada, for patients possessing a cervical intraepithelial neoplasia (CIN) grade II or III lesion, this entails a 6-month follow-up examination and subsequent biopsy (Bentley J *et al.*, 2012). For lesions that do not regress, the physician may decide to perform a loop electrosurgical excision procedure (LEEP) to remove the dysplastic tissue. Unfortunately, lesions can recur in as many as 30% of cases (Gonzalez *et al.*, 2001). The prevalence of these actively surveyed lesions remains an untapped temporal window for treatment. It would seem prudent to develop a non-invasive antiviral therapy that could reduce lesion grade, reduce colposcopy visits, and/or reduce the number of surgical interventions. One possible treatment would be the use of RNA interference (RNAi), which targets mRNA transcripts for degradation, abrogating a gene's ultimate translation (described below). RNAi is an active area of research for many therapeutics, but is particularly alluring for HPV infection because the viral genes are foreign, and in theory, employing RNAi would have minimal effect on healthy cells, or on host gene regulation (Jiang and Milner, 2002). In theory, utilizing RNAi to reduce E6 expression could restore cellular p53, potentially inducing apoptosis in HPV-infected cells while leaving healthy cells unharmed (Togtema *et al.*, in press).

1.1.6 RNA interference and off-target effects

RNA interference is an ancient and conserved viral defence mechanism present in plants and animals (Fire *et al.*, 1998; Waterhouse *et al.*, 1998). The process of RNAi involves the Dicer-mediated cleavage of double-stranded RNA molecules into short oligonucleotides approximately 21-23 nt in length (**Figure 3**). These short oligonucleotides – or small-interfering RNA (siRNA) – are then incorporated into the RNA-induced silencing complex (RISC). The activated RISC complex then unwinds the double-stranded siRNA, retaining the anti-sense strand (or guide-strand) which is used for targeting mRNA transcripts that possess guide-strand complementarity (Nykanen *et al.*, 2001). If the target transcript has limited complementarity to the guide-strand, translation of that transcript may be inhibited. If the target transcript has near perfect complementarity, the transcript will be cleaved by RISC, and subsequently degraded (Hammond *et al.*, 2000). Importantly, these siRNA molecules can be processed from double-stranded RNA produced from host transcripts, foreign viral genes/genomes, or synthetic oligonucleotides. Therefore, it is possible to rationally design and exogenously introduce siRNA to target any gene for silencing.
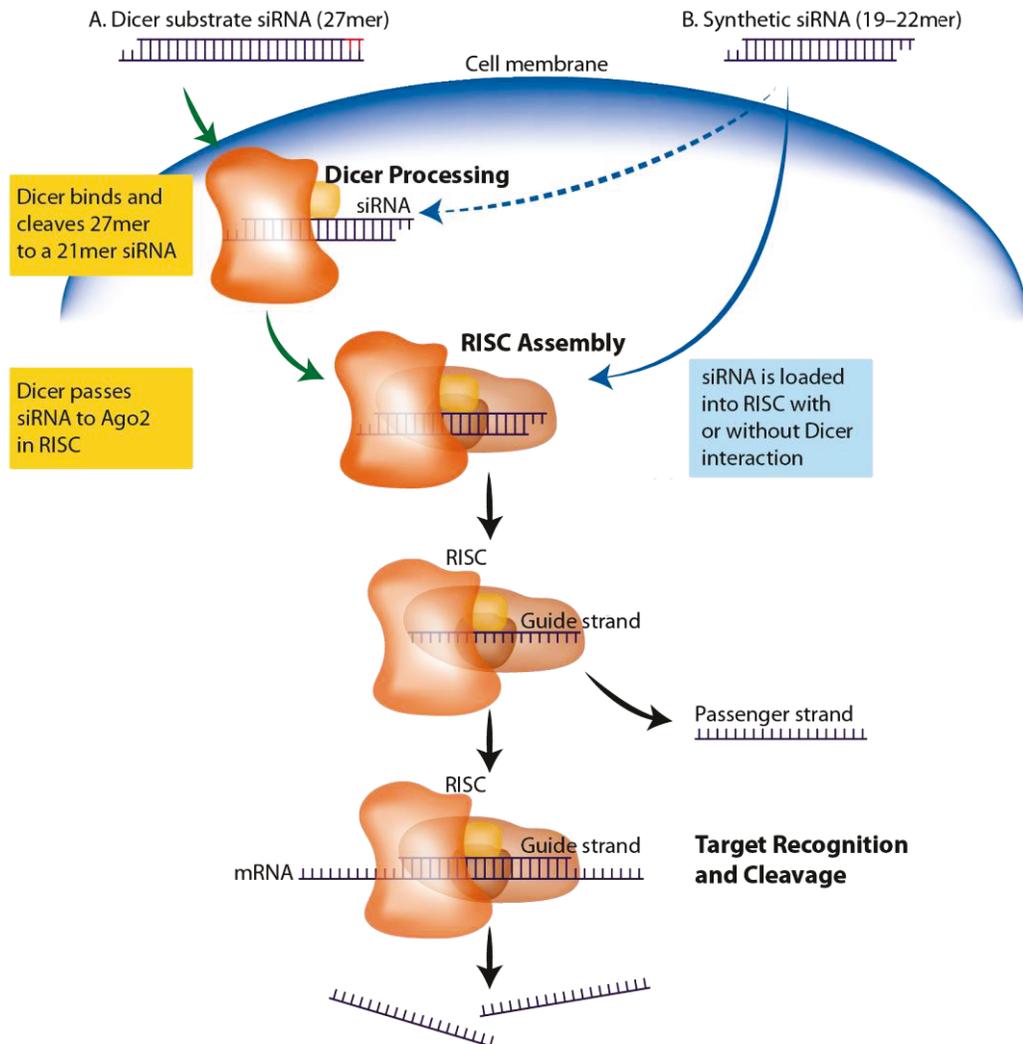
Figure 3. Schematic representation of RNAi with siRNA and DsiRNA. Canonically, Dicer processes double-stranded RNA into 21-23 nt fragments. Oligonucleotides can be created that simulate Dicer substrates, or siRNA molecules can be introduced that feed directly into RISC. Image source: http://kemomed.si/en/products/3-reagents-and-consumables/26-Integrated+DNA+Technologies/141-Gene+Silencing

One concern when using siRNA is the potential for off-target effects. Though the definition of 'off-target effect(s)' varies significantly, in its broadest sense it includes: 1) the effects from siRNA delivery mechanisms; 2) siRNA-mediated innate immune activation (Jackson *et al*., 2006); and 3) other unintended changes in host gene expression (Hanning *et al.*, 2013). The latter-most typically describes host transcripts that are degraded due to significant sequence complementarity with the siRNA guide strand. Many of these

off-target transcripts can be avoided when designing siRNA oligonucleotides, and algorithms exist to predict which host transcripts possess complementarity to siRNA oligonucleotides. However, these algorithms are typically designed to predict host transcripts that possess near-perfect guide-strand complementarity, and off-targets predicted *in silico* match poorly with those found *in vitro* (Hanning *et al.*, 2013). Indeed, studies have used bioinformatic approaches to show that very few – if any – off-target gene transcripts possess significant sequence complementarity to the guide strand (Jackson *et al.*, 2003). In fact, only a subset of down-regulated transcripts possess any appreciable complementarity to the guide-strand, and these transcripts contain sequence complementarity to bases 2 through 8 of the guide strand, termed the 'seed region'. More specifically, these repressed genes were found to contain seed region complementarity within their 3' untranslated region (UTR). Importantly, although 3'-UTR seed matches are a robust predictor for off-target effects, they only account for a fraction of transcriptional changes observed in response to a given siRNA oligonucleotide (Birmingham *et al.*, 2006). This lack of overall predictability merits transcriptomic analysis when elucidating the off-target effects of any novel siRNA oligonucleotide.

Transcriptomic analysis is both expensive and cumbersome, and employing such techniques on every siRNA oligonucleotide would be overwhelming. Practically speaking however, it is not always necessary to assess *all* of the off-target effects, but merely to demonstrate that the desired cytological/physiological effects are due to the siRNA treatment. For many researchers, siRNA oligonucleotides of therapeutic interest are meant to induce apoptosis in a diseased or cancerous cell, while inflicting minimal harm on healthy cells. In this scenario, it is most prudent to demonstrate that apoptosis is due to the

knock-down of the desired gene. When assessing off-target effects in target cells, an oligonucleotide very similar in sequence to the query siRNA ought to be used. The C9/11 control is a rationally designed siRNA control, whereby bases 9 through 11 on the query siRNA are altered (Buehler *et al.*, 2012). These base alterations abolish target knock-down, while maintaining the vast majority of sequence-specific off-targets. It does this in part by retaining the seed-region sequence of the query siRNA. The C9/11 control is therefore superior to scrambled siRNA controls.

1.1.7 Previous work in RNA interference

In previous work, our research group compared the knock-down efficiency of different oligonucleotides designed to target the E6 transcript, with the aims of finding a highly potent molecule for abrogating E6 translation, and ultimately restoring p53 (MSc Thesis, Jessica Grochowski, 2015; Togtema *et al.*, in press). Oligonucleotides were designed to target the E6 splice-site on the E6/E7 transcript, which successfully inhibits E6 translation but retains translation of E7 (Smotkin *et al.*, 1989). In effect, this should restore p53 levels in the presence of the proliferation-promoting E7, which is believed to drive infected cells towards apoptosis (McLaughlin-Drubin, 2012). Our lab compared Dicer-substrate RNA (DsiRNA) to siRNA oligonucleotide molecules that possess the same target sequence. In brief, a DsiRNA oligonucleotide feeds into the RNAi pathway further upstream than siRNA. As DsiRNA molecules can be significantly more potent than their siRNA counterparts (Kim et al, 2005), a DsiRNA molecule was developed based upon a corresponding siRNA, to draw direct comparisons. The target sequence within the E6 splice site was designed using the Rosetta algorithm (Rosetta Inpharmatics Inc.), and we found that when tested in the HPV16 cervical cancer cell lines CaSki and SiHa, Rosetta

DsiRNA performed better than Rosetta siRNA. **Figure 4** summarizes the results obtained from previous work using Rosetta DsiRNA. Maximum E6 knock-down occurred between 10 nM and 250 nM, with no statistical difference between these concentrations. There was no statistical difference between incubation times, though 48 appeared maximal for both CaSki and SiHa.
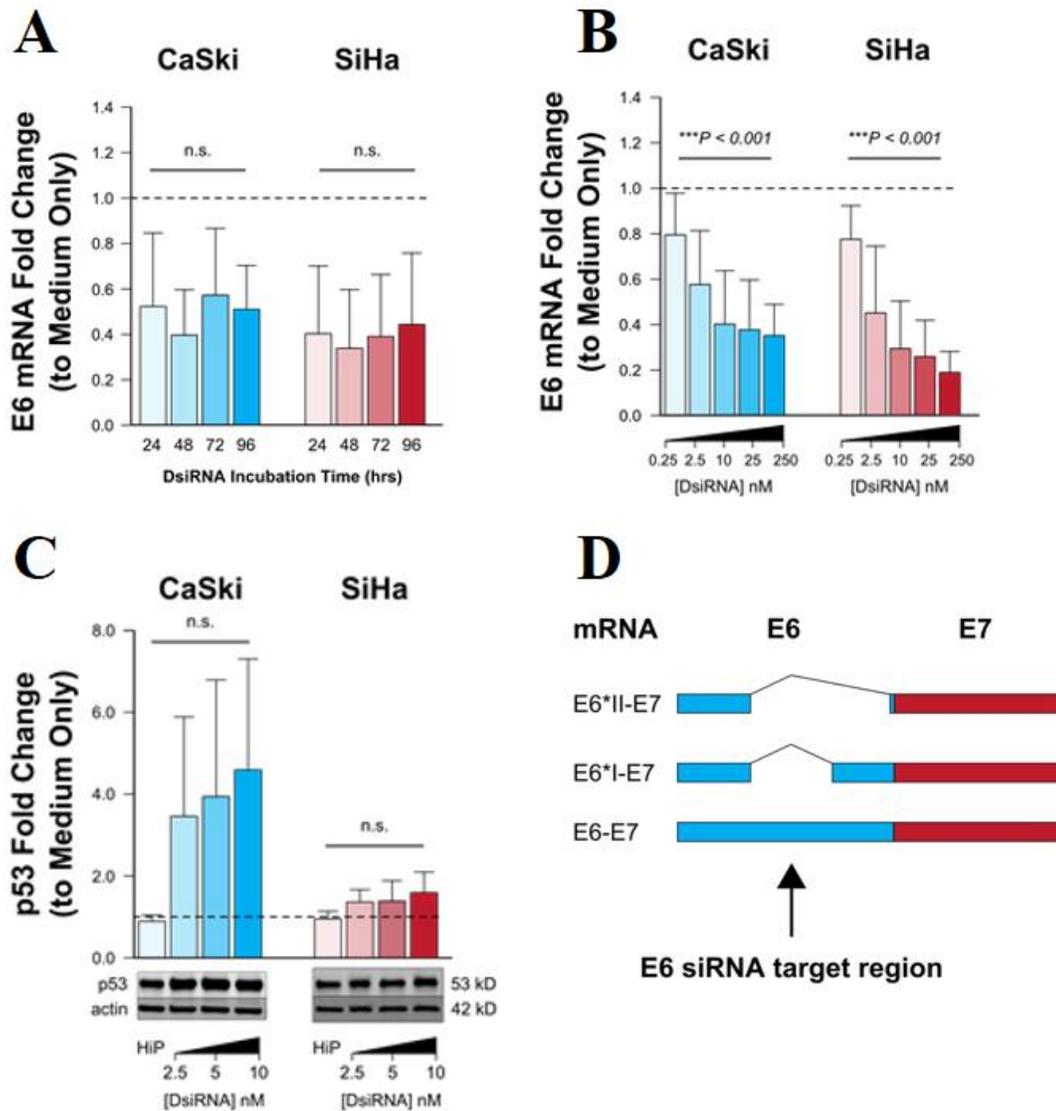
Figure 4. Overview of previous results obtained from E6 knock-down with Rosetta DsiRNA. No significant difference between incubation time was found for either cell type (n=3, **A**). Knock-down of E6 was maximal between 10 nM and 250 nM of DsiRNA (n=3, **B**), though there was no significant difference found between these concentrations. Knock-down of E6 restored p53 as determined by Western blot, though these results were highly variable and not statistically significant (n=5, **C**). Diagram of the RNAi target site within the E6 transcript (**D**). Figure created by Robert Jackson, PhD Candidate, modified from Togtema *et al*., (in press).

1.2 Research rationale

When studying HPV in the laboratory, primary neonatal foreskin keratinocytes are often employed. Though these keratinocytes are permissive to the viral life cycle (Flores *et al*., 1999), HPV16 is not associated with carcinoma of skin keratinocytes. Utilizing cervical keratinocytes from patient-derived cultures is not only a more accurate model to the disease in question, but it also permits the modelling of patient variability. Since culturing cells from patient biopsies and creating organotypic cultures is not a trivial task, the goal of this work is simply to develop methods to do so. Similarly, because we wish to develop RNAi therapeutics, patient-derived cells can not only be utilized to model patient-specific responses, they would also be more accurate models than the highly transformed immortalized cancer cell lines. Based on our previous work on DsiRNA E6 knock-down in HPV16 cancer cell lines (Togtema *et al.*, in press), we would like to continue our experimental algorithm by assessing the downstream effects of E6 knock-down, at the level of gene expression, viability, and apoptosis.

1.3 Hypotheses

Given the results of Schweinfurth *et al*. (2006) and Liu *et al*. (2016), and the potential issues listed by Stanley (2002), we expect:

1. Roughly 10-30% of established cultures will succumb to microbial contamination.

2. The longest cultures will grow for 6 to 8 weeks.

3. After utilising 5-10 samples to establish our methodology, we may see a 30% success rate in establishing cultures.

In previous work, we assessed E6 knock-down in HPV16 positive cancer cell lines, and found that p53 restoration was limited in SiHa, and highly variable in CaSki (**Figure 4**). Additionally, there was no statistical difference in E6 knock-down between 10 nM and 250 nM DsiRNA treatments. Therefore, we utilized DsiRNA between 2.5 nM and 10 nM for further experiments. This concentration range was also believed to span the median inhibitory concentration, as well, these lower concentrations are considered more clinically relevant (Persengiev *et al*., 2004). Despite 10 nM providing near-maximal E6 knock-down, it may still be insufficient to restore cellular processes. We will also include a C9/11 DsiRNA for a control, but overall we may expect:

1. hTERT levels will decrease because E6 levels are notably reduced.

2. E7 levels will remain relatively unchanged, as Rosetta DsiRNA targets the splice site.

3. Downstream effects of p53 restoration will be unchanged from controls.

4. Cellular viability and growth will be unchanged.

1. Materials and Methods

2.1 Materials and methods for downstream effects of E6 knock-down

2.1.1 Cell culture and maintenance

Cell cultures were maintained in a humidified incubator at 37°C with 5% CO_2. The cervical cancer cell lines CaSki (ATCC, Cat. No. CRL-1550) and SiHa (ATCC, Cat. No. HTB-35) were cultured in Dulbecco's Modified Eagle's Medium (DMEM; Fisher Scientific, Cat. No. SH30243.01) containing 10% heat-inactivated fetal bovine serum (FBS; Fisher Scientific,

Cat. No. SH30396.03) and 1X antibiotic/antimycotic (Fisher Scientific, Cat. No. SV3007901). When passaging cultures, cells were washed with Dulbecco's Phosphate Buffered Saline (DPBS; Fisher Scientific, Cat. No. SH30028.02) before adding 2 ml of 0.05% trypsin containing 0.02% ethylenediaminetetraacetic acid (Trypsin-EDTA; Fisher Scientific, Cat. No. SH3023602), and incubated at 37°C for 5-10 minutes until cells were sufficiently detached. At which point, 4 ml of culture media was added to inactivate the trypsin. Cultures were seeded at 10% confluency and maintained up to 80% confluence before subsequent passaging.

2.1.2 Cryogenic storage and retrieval

When preparing stocks for cryogenic storage, cells were trypsinized as described and quantified using a TC10™ Automated Cell Counter (Bio-Rad, Cat. No. 145-0009). Cells were then pelleted at 750 rpm for 5 minutes, and then resuspended in the appropriate volume of 90% DMEM-FBS and 10% dimethyl sulfoxide (DMSO; Sigma-Aldrich, Cat. No. 34869) to achieve 1×10^6 cells per ml, preparing 1 ml stocks. Stocks were then frozen using a controlled-rate cooling container (Thermo Fisher Scientific, Cat. No. 5100-0001) at -80°C. Frozen vials were subsequently stored in liquid nitrogen for long-term use.

When retrieving cell stocks from cryogenic storage, vials were thawed to room temperature and added to 4 ml of DMEM-FBS. The cells were pelleted at 750 rpm and the media was aspirated. Cell pellets were re-suspended in 10 ml of media and plated onto T-75 flasks for incubation.

2.1.3 Mycoplasma testing

Cultures of CaSki and SiHa cells were regularly tested for *Mycoplamsa* contamination by fluorescent staining with 4'-6-diamidino-2-phenylindole (DAPI). Approximately 1×10^4 cells were seeded onto sterile glass cover slips (Thermo Fisher Scientific, Cat. No. 12-541A) and grown in 35mm cultures dishes for 2-3 days. At which point, the media was removed and cells were fixed using Carnoy's fixative (3:1 solution of methanol (Thermo Fisher Scientific, Cat. No. A4544) and glacial acetic acid (Sigma-Aldrich, Cat. No. 695092-2.5L), respectively). Fixative was first added to cells for 5 minutes, the fixative was then removed, and fresh fixative was added for another 10 minutes. The cover slips were removed and allowed to air dry. Cover slips were then mounted on a microscope slide using Vectashield Mounting Medium containing DAPI (1.5 µg/mL, Vector Laboratories. Cat. No. H-1200). This method stains the DNA of *Mycoplasma* thereby permitting their visualization within the cytoplasm of infected cells via fluorescent microscopy.

2.1.4 C9/11 design and validation

A control DsiRNA was designed in which bases 9 through 11 of the guide strand were altered to create three consecutive mismatches against the E6 transcript: termed the C9/11 control (Buehler *et al.*, 2012). It has been shown that a single base mutation at nucleotides in the 9th, 10th, 11th, or 12th position can abolish target-mRNA knock-down by up to 90% (Birmingham *et al.*, 2006). By combining three consecutive mismatches, it can be ensured that target sequence knock-down is abolished, and off-targets are retained. This C9/11 control siRNA can then be used as a direct comparison for the observed downstream effects, such as apoptosis. This instills confidence in scientific results that typical

scrambled control siRNA cannot (Buehler *et al*., 2012). Each mismatch-causing nucleotide was selected based off of its ideal knock-down abrogating potential as described in Birmingham *et al.* (2006).

The Rosetta DsiRNA pre-processing guide-sequence 5'-AUCUCUAUAUACUAUGCAUAAAUCCCG-3' was changed to sequence 5'-AUCUCUAUAUACUA<u>ACA</u>AUAAAUCCCG-3', underlining to indicate base changes. To validate that the C9/11 control has abrogated E6 knock-down, CaSki and SiHa cells were seeded into T-25 flasks and transfected with the C9/11 DsiRNA. Cell culture, transfection, harvesting, and RT-qPCR analyses were performed using parameters described below.

2.1.5 Chemical transfections and cell harvesting

Cells were seeded into T-25 flasks at 3.5×10^5 cells per flask for CaSki, and 1.5×10^5 cells per flask for SiHa. After 24 hours, the media was changed with 4 ml of fresh DMEM-FBS, and cultures were transfected with DsiRNA complexes to a final concentration of 2.5, 5 or 10 nM of Rosetta E6 DsiRNA or the corresponding C9/11 control DsiRNA. Transfection complexes consisted of 1 ml total of serum-free DMEM, the corresponding oligonucleotide, and HiPerFect (Qiagen, Cat. No. 301707) added according to the manufacturer's instructions. The solution was vortexed for 10 seconds and subsequently incubated at room temperature for 10 minutes, prior to drop-wise addition to cultures. The cells were harvested 48 hours after transfection, with one quarter from each flask used for RT-qPCR analyses of E6, E7, hTERT and p21[WAF1/CIP1] mRNA expression, and the remaining three-quarters being stored for future Western blot analysis. Cell pellets

were washed with DPBS and stored at -80°C until RNA extraction was performed.

2.1.6 RNA extraction and reverse transcription real-time PCR (RT-qPCR) analysis

Relative quantification of E6, E7, hTERT, and p21$^{WAF1/CIP1}$ gene expression was determined using reverse-transcription quantitative polymerase chain reaction (RT-qPCR). Total RNA was extracted from cell pellets using the RNeasy Plus Mini kit (Qiagen, Cat. No. 74136), according to the manufacturer's instructions. RNA quantity and integrity were assessed using the Experion Automated Electrophoresis system and RNA StdSens Analysis kit (Bio-Rad, Cat. No. 7007013). Reverse transcription into cDNA was done using the High-Capacity cDNA Reverse Transcription kit (Fisher Scientific, Cat. No. 4368814). RT-qPCR reactions consisted of 150 ng of cDNA, 45 µL of TaqMan® Universal PCR Master Mix (Thermo Fisher Scientific; Cat. #: 4364338), 4.5 µL of appropriate TaqMan® Gene Expression Assay and nuclease-free water for a final volume of 90 µL. Triplicate reaction volumes of 25 µL for each sample were loaded into transparent 96-well plates and analyzed using a 7500 ABI real-time thermocycler. Hypoxanthine phosphoribosyltransferase 1 (HPRT1) was chosen as a stable reference gene based on previous experiments (DeCarlo *et al.*, 2008). Relative expression was calculated using the 2$^{-\Delta\Delta CT}$ Livak analysis method (Livak and Schmittgen, 2001; Bustin *et al.*, 2009). Statistical comparisons were done via a one-way ANOVA.

Table 1. List of qPCR probes used in gene expression analysis.

Taqman Gene Assay	Assay ID
Full-length HPV16 E6	AI0IW1V (Custom)
HPV16 E7	AIBJW6W (Custom)
hTERT	Hs00162669_m1
p21$^{WAF1/CIP1}$	Hs01040810_m1
HPRT1	Hs99999909_m1

2.1.7 MTT cell viability assay

Cell viability was measured via the MTT assay (Mosmann, 1983). Cellular metabolic activity is indirectly measured through a colorimetric assay, where tetrazolium salts (yellow) are reduced to formazan (purple), in a manner quantitative to cell numbers and/or viability. CaSki and SiHa cells were trypsinized and seeded into 24-well plates at 2 x 10^4 cells per well. After 24 hours, cells were transfected with 200 µl of complexes using HiPerFect chemical transfection reagent following the manufacturer's instructions. Treatments consisted of DsiRNA and C9/11-DsiRNA at concentrations of 2.5, 5, and 10 nM; with a media-only control. After 48 hours, 25 µL of 5 mg/mL 3-(4,5-Dimethyl-2-thiazolyl)-2,5-diphenyl-2H-tetrazolium bromide (MTT; Sigma-Aldrich, Cat. No. M5655) was added to each well and incubated at 37°C for 4 hours. The cell culture media was then aspirated, and tetrazolium crystals were solubilized with 100 µL 0.1 N HCl (Sigma Aldrich, Cat. No. 320331) in isopropanol (Fisher Scientific, Cat. No. HC5001GAL). Absorbances were measured at 570 nm subtracting background at 650 nm using a BioTek® Powerwave XS Plate Reader. Each biological replicate (n=4) was performed in technical triplicate. For each biological replicate, absorbances amongst technical replicates were averaged, and normalized to the average absorbance of the media-only control. Standard deviation was calculated across the average relative absorbances.

2.1.8 Cell-cycle and apoptosis assays

CaSki and SiHa cells were trypsinized and seeded into 6-well plates at 1 x 10^5 cells per well. After 24 hours, the media was changed, and cells were transfected as described previously, with Rosetta DsiRNA or C9/11 DsiRNA at 2.5 nM, 5 nM, and 10 nM. Cultures

were treated for 48 and 96 hours. Floating and adherent cells were harvested, pelleting at 750 rpm for 5 minutes. Cell pellets were resuspended in 5 ml of DPBS and again centrifuged for the first wash. Upon resuspension for the second wash, harvested cells were divided equally between cell-cycle and apoptosis assays and again pelleted. Cell pellets for apoptosis assays were processed immediately for flow cytometry (described below). Cell pellets for cell-cycle analysis were fixed by adding 1 ml of 70% ethanol to pellets while vortexing (Fisher Scientific, Cat. No. HC11001GL). Fixed cells were stored at 4°C until analysis was performed. Data was obtained using a FACSCalibur flow cytometer, utilizing BD CellQuest software.

Apoptotic assays we performed using an Annexin V FITC Kit (Trevigen, Cat. No. 4830-01-K), as per kit instructions. During apoptosis, phosphatidyl serine flips to the outer membrane of the cell (Fadok *et al*., 1992), and this phosphatidyl serine can be bound by Annexin V in a calcium-dependant manner (Tait and Gibson, 1992). In turn, fluorescently-tagged Annexin V can be used to label apoptotic cells for flow cytometry analysis (Koopman *et al.*, 1994). Briefly, cells were washed with 1X Binding Buffer and resuspended in 100 µl of Annexin V Incubation Reagent containing propidium iodide and Annexin V-FITC in 1X Binding Buffer. Following a 15-minute incubation, 400 µl of 1X Binding Buffer was added and cells were apoptotic events were counted by flow cytometry.

For cell-cycle analysis, the fixed cells were removed from 4°C storage and pelleted as previous. Ethanol was decanted, and the cells were then washed in 1X PBS and resuspended in propidium iodide staining solution (0.1% Triton X-100, 10 µg/mL RNase cocktail, 20 µg/mL propidium iodide in 1X PBS). After a 30-minute incubation, cells were analyzed by flow cytometry (Shapiro 1988).

Samples were run on a BD FACSCalibur flow cytometer with BD CellQuest™. Software. Events were analyzed using Flowing Software 2, and statistical analysis was performed in R version 3.2.3 (R Core Team, 2013) within R Studio (RStudio Team, 2015). Samples were prepared for flow cytometry by Peter Villa, with flow analyses and statistical analyses performed by PhD candidate Robert Jackson. Software work-flow of apoptosis analyses and cell-cycle analyses are illustrated in **Figure A1** and **Figure A2**, respectively.

2.1.9 Cell growth analysis

CaSki and SiHa cells were seeded into T-25 flasks at 2×10^5 cells per flask. After 24 hours, cultures were transfected with DsiRNA complexes prepared using HiPerFect chemical transfection reagent according to the manufacturer's instructions. Cultures were treated with Rosetta DsiRNA or the corresponding C9/11 control DsiRNA at a final concentration of 10nM. Untreated cultures and cultures treated with the transfection reagent only were used as controls. When control cultures reach confluency, all cultures for the respective cell type were trypsinized and cell numbers were recorded via a Bio-Rad® TC10™ Automoated Cell Counter, replating 2×10^5 cells per flask. Cultures were transfected 24 hours after each replating, and were subsequently monitored for 17 days. Culture doublings were calculated using:

$$\text{(number of cells seeded)} \times 2^n = \text{(final cell count)}$$

Cumulative culture doublings were expressed from summation across passages.

2.2 Methods for culturing cervical keratinocytes

2.2.1 Human research ethics and clinical services

This study was approved by the Research Ethics Boards (REB) at Lakehead University (#019 16-17) and the Thunder Bay Regional Health Sciences Centre (TBRHSC; #2016107), according to Tri-Council Policy Statement 2 (2014) on human research ethics. Application to the REB required drafts of the: 1) logistical and laboratory protocols; 2) consent form; 3) brief study budget; 4) REB application template, involving risks and logistics; and 5) conflicts of interest. Studies must first be registered with the Clinical Research Services Department (CRSD) at TBRHSC prior to their application to the REB (**Figure 5**), which meets monthly. This study was registered December 2015, and upon submission to the REB at TBRHSC, major revisions were requested in February of 2016. The application was re-submitted in March (2016), where minor revisions were requested, appended, and approved in April (2016). The application was then sent to Lakehead University in May (2016), where minor revisions were again requested and approved by June (2016), and subsequently amended at TBRHSC in July of 2016. The project then commenced in August of 2016 – over 8 months after registration.

For the second phase of this study – which included patient chart review and altered laboratory protocols – an amendment was requested in June of 2017, after the study was renewed and the summary of the initial results was provided to the REB. This amendment was granted through both institutions and the acquisition of samples began again in July of 2017.

Other requests were made through CRSD for additional services. Prior to study commencement, CRSD ensured the appropriate training of the affiliated nurses so that they

may consent patients to participate in this study. For the second phase of this study, CRSD also facilitated a service contract between TBRHRI and TBRHSC-Pathology Services to paraffin-embed the 3D raft cultures and prepare slides for immunohistochemistry. Pathology Services provided 4 μm Haemotoxylin and Eosin (H&E) stained raft sections for this project, as well as additional unstained slides upon request.
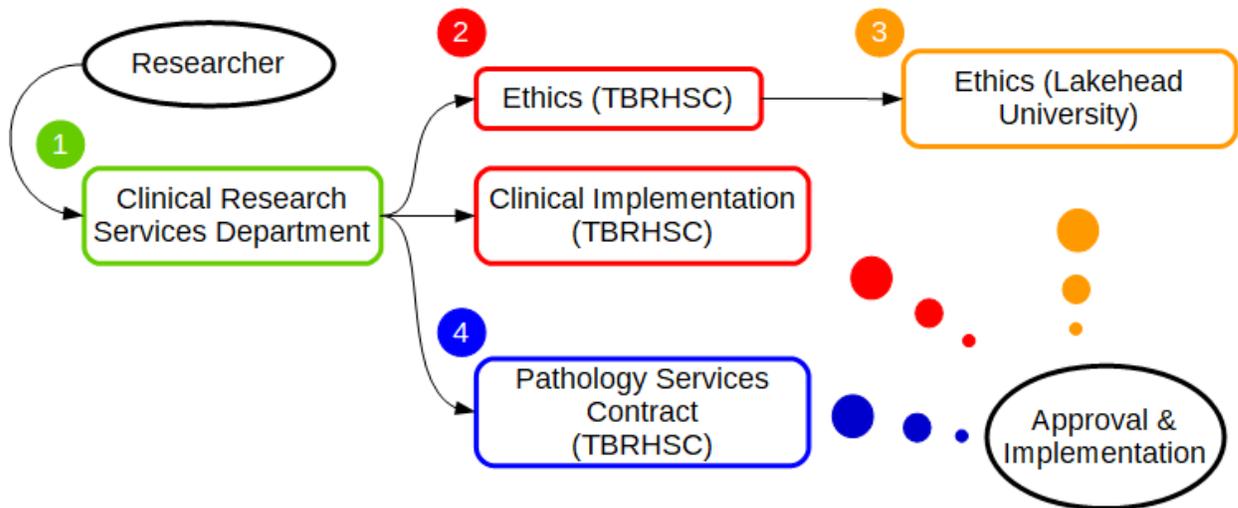
Figure 5. Schematic representation of the application process for receiving approval of a clinical research project. Projects are first registered with the Clinical Research Services Department (CRSD) at the Thunder Bay Regional Health Sciences Centre (TBRHSC) (**1**). Applications can then be sent to the Research Ethics Board (REB, **2**); consisting of literature, scientific merit, laboratory protocols, staff training, and logistics of clinical implementation. Once approved, the application is sent to the REB at Lakehead University (**3**). Once approved by both the hospital and university, the study can commence. Further services are contracted through CRSD (**4**).

2.2.2 HPV typing

Prior to their colposcopic examination, study participants had a swab of their cervix taken, which was to be sent to the Public Health Agency of Canada if they donated a biopsy specimen for this study. HPV typing was provided in kind by Dr. Alberto Severini at the National Microbiology Laboratory. In brief, a Luminex sequencing platform was used to

detect potential HPV type(s) present. HPV DNA was amplified using nested-PCR, and probes specific for 45 different mucosal HPV types were used to detect the HPV type(s) present (Zubach *et al.*, 2007). This method is capable of detecting multiple HPV types present in a single sample.

2.2.3 Culture maintenance

Cell cultures were maintained in a humidified incubator at 37°C with 5% CO_2. The immortalized mouse embryonic fibroblast cell line J2 3T3 (Allen-Hoffmann *et al.*, 2000) and primary human foreskin fibroblasts (ATCC, Cat. No. CRL-2097) were cultured in Dulbecco's Modified Eagle's Medium (DMEM; Fisher Scientific, Cat. No. SH30243.01) containing 10% heat-inactivated fetal bovine serum (FBS; Fisher Scientific, Cat. No. SH30396.03) and 1X antibiotic/antimycotic (Fisher Scientific, Cat. No. SV3007901). When passaging cultures, cell monolayers were washed with Dulbecco's Phosphate Buffered Saline (DPBS; Fisher Scientific, Cat. No. SH30028.02) before adding 2 ml of 0.05% trypsin containing 0.02% ethylenediaminetetraacetic acid (Trypsin-EDTA; Fisher Scientific, Cat. No. SH3023602), and incubated at 37°C for 5-10 minutes until cells were sufficiently detached. At which point, 4 ml of culture media was added to inactivate the trypsin. Cultures were seeded at 10% confluency and maintained up to 80% confluence before subsequent passaging.

2.2.4 Isolation and culture of keratinocytes from cervical biopsy specimens

Cultures were established via a modified Liu *et al.* (2016) method. Biopsy specimens were taken by the physician using a Tischler Morgan Biopsy forceps with a 3

mm x 7 mm bite (**Figure 6**). Biopsy specimens were placed in 5 ml of transport media, consisting of serum-free DMEM containing 20X antibiotic/antimycotic with 50 µg/ml gentamicin (Sigma Aldrich, Cat. No. G1914), and stored at 4°C for several hours until processing. Samples were then washed 5 times with 1 ml of DPBS containing 20X antibiotic/antimycotic and 50 µg/ml gentamicin. Washed specimens were placed in 1 ml of 0.2% Type I Collagenase (Fisher Scientific, Cat. No. 17100017) in 1X Hank's Balanced Salt Solution (HBSS; Sigma Aldrich, Cat. No. H4385) containing 3 mM calcium chloride and 1mM magnesium chloride, without carbonate. Samples were minced with curved iris scissors and incubated on a shaker at 37°C and 225 rpm for 1 hour. Digested specimens were washed twice with 10 ml of DPBS, pelleted at 750 rpm for 5 minutes, and re-suspended in 2 ml of keratinocyte media containing 5% FBS and 1X antibiotic/antimycotic. Re-suspended tissue digests were plated onto a collagen- and FBS-coated T-12.5 flask. Tissue culture flasks were coated using the Coating Matrix Kit (Fisher Scientific, Cat. No. R011K) as per kit instructions, and then coated with 2 ml FBS for 2-3 hours. After 4 to 5 days, the non-adherent tissue pieces were removed and the media was replaced with serum-free media.

Figure 6. Tischler Morgan biopsy forceps. Typical forceps utilized by colposcoptists to acquire cervical biopsy specimens. Forcep bite of 3 mm wide and 7 mm long. Source: https://homeoftech.en.ecplaza.net/products/morgan-tischler-biopsyforceps_2787756

In the first phase of this study ('Phase I'), where methods were developed to culture cervical keratinocytes in-house, cervical cells were cultured in Keratinocyte Serum-Free Growth Medium (KGM; Cell Applications, Cat. No. 131-500). By contrast, in the second phase of this study ('Phase II'), we aimed to increase the *in vitro* lifespan of keratinocytes by replacing the cell culture media with EpiLife basal media (Fisher Scientific, Cat. No. MEPI500CA) supplemented with Human Keratinocyte Growth Supplement (Fisher Scientific, Cat. No. S0015). Unlike most keratinocyte media, this formulation contains recombinant human insulin-like growth factor-I (IGF-I) in place of insulin, which helps to reduce differentiation and increase the lifespan of keratinocytes *in vitro*. IGF-I possesses more mitogenic potential than insulin, as it activates more cellular receptors than insulin;

where IGF-receptors also interact with intracellular adaptor proteins more effectively than insulin receptors (Sasaoka *et al*., 1996; **Figure 7**). In turn, IGF-I is 10-50 times more potent than insulin at activating MAPK in keratinocytes (Neely *et al*., 1991), which also has the effect of increasing their *in vitro* lifespan. The basal media also contains a reduced calcium concentration to prevent cellular differentiation. In addition, Y-27632 was added to the media as a chemical inhibitor of Rho-associated protein kinase (ROCK). This drug has been shown to drastically increase the lifepsan of keratinocytes in vitro (Strudwick *et al*., 2015). Inhibition of ROCK reduces expression of down-stream targets for p53, which is thought to be a major mechanism by which Y-27632 promotes longevity. As well, ROCK-inhibition has been shown to synergize with E6, and promote drug-dependant cellular immortalization of keratinocytes without the need for E7 (Dacik *et al*., 2016).

Once cultures were established, keratinocytes were maintained at 10% to 80% confluence between passages. Cultures were split using 2 ml of Trypsin-EDTA, whereby trypsin was inhibited with 3 ml of Trypsin Neutralizing Solution (Cell Applications, Cat. No. 080-100). The cells were centrifuged at 750 rpm for 5 minutes, where the neutralized trypsin solution was removed, and cells were re-suspended in fresh cell culture media (i.e. KGM or EpiLife with Y-27632, for Phase I and Phase II, respectively). Cells were counted using a BioRad TC-10^{TM} Automated Cell Counter. New flasks were coated with collagen for each successive passage.
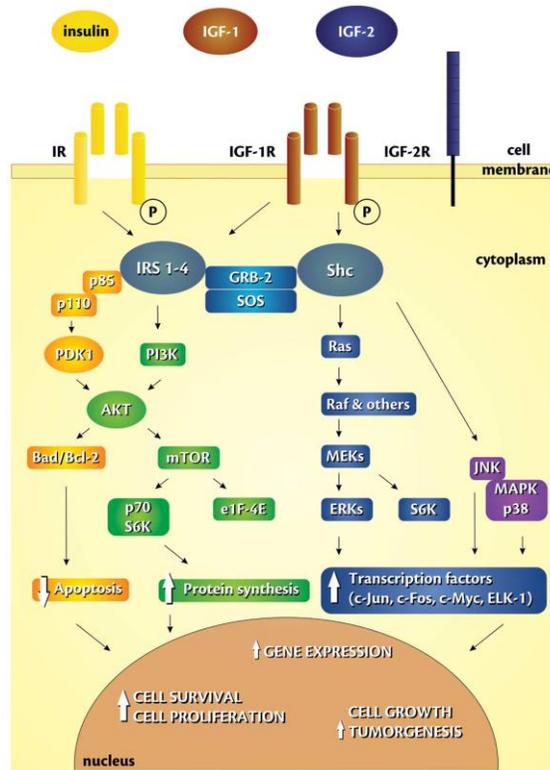
Figure 7. Signalling pathway of Insulin and Insulin-like Growth Factors. Insulin-like Growth Factors (IGFs) possess greater mitogenic potential than Insulin signalling, where IGF-receptors interact with Shc/Grb2/Sos more effectively than insulin-receptors (Sasaoka *et al*., 1996), and activate MAPK in keratinocytes with greater potency than insulin (Neely *et al*., 1991). Image Source: <https://www.spandidos-publications.com/10.3892/ijo.2012.1666>

2.2.5 Mycoplasma testing

Primary cell cultures were tested for M*ycoplasma* indirectly by using the J2 3T3 fibroblast cell line as an indicator cell line. In this method, the J2 cells are cultured in media from the cell line in question (i.e. the primary cervical cells), in order to infect the indicator cell line. It is commonly observed that *Mycoplasma* replicate at a much lower rate and at lower titres in primary cells, which may cause ambiguous or delayed results when trying to observe *Mycoplasma* directly within the cell's cytoplasm. Therefore, an indicator cell line that is highly permissive to *Mycoplasma* infection and replication is utilized, such as

the J2 cell line (McGarrity and Barile, 1983). These J2 cells were cultured in conditioned media from cervical cell cultures were tested for *Mycoplamsa* contamination by fluorescent staining with 4'-6-diamidino-2-phenylindole (DAPI). This method stains the DNA of *Mycoplasma* thereby permitting their visualization within the cytoplasm of infected cells via fluorescent microscopy. Approximately 1 x 10^4 J2 cells were seeded onto sterile glass cover slips (Thermo Fisher Scientific, Cat. No. 12-541A) and grown in 35mm cultures dishes in 3 ml of media consisting of 2 ml DMEM-FBS with antibiotic/antimycotic, and 1 ml of conditioned media. After 3 days, the media was removed and cells were fixed using Carnoy's fixative [3:1 solution of methanol (Thermo Fisher Scientific, Cat. No. A4544) and glacial acetic acid (Sigma-Aldrich, Cat. No. 695092-2.5L), respectively]. Fixative was first added to cells for 5 minutes, whereby the fixative was then removed, and fresh fixative was added for another 10 minutes. The cover slips were then removed and allowed to dry. Cover slips were then mounted on a microscope slide using Vectashield Mounting Medium containing DAPI (1.5 µg/mL, Vector Laboratories. Cat. No. H-1200).

2.2.6 Construction of organotypic raft cultures

Early passage primary human foreskin fibroblasts were cultured as described previously, and low passage (P<5) human fibroblasts were used in the preparation of dermal equivalents. Fibroblasts were trypsinized and counted, and 1 x 10^6 cells were pelleted and re-suspended in 2 ml FBS. Using a sterile 50 ml beaker with a magnetic stir bar, cooled in ice atop a magnetic stir plate, 7.5 ml of type I rat tail collagen (~4.00 mg/mL; Millipore, Cat. No. 08-115) and 1 ml of 10X HBSS was added and thoroughly mixed. The solution was neutralized using 5 µl increments of 5 *N* NaOH, requiring ~30 µl in total.

Once neutralized, the fibroblasts were immediately added and thoroughly mixed. Dermal equivalents were then prepared by pipetting 500 µl of the collagen-cell suspension into wells of a 48-well plate (yielding ~5 x 10^5 fibroblasts per dermal equivalent). The dermal equivalents were then incubated for ~30 minutes at 37°C, where they would solidify. Afterwards, 500 µl of DMEM-FBS was added to the top of each raft and incubated overnight.

Rafts were prepared in technical triplicate for each patient culture. For each raft, 2.5 x 10^5 keratinocytes were needed to create the basal layer of the epidermis. Keratinocytes were trypsinized and re-suspended to yield 5 x 10^6 cells/ml, so that the desired cell number could be seeded on top of rafts in a 50 µl cell suspension. Keratinocytes were re-suspended in media consisting of equal parts EpiLife Media and NIKS Complete Media. NIKS Complete media was prepared containing 3 parts Ham's F-12 media (Invitrogen, Cat. No. 21700-075) to 1 part DMEM; supplemented with 2.5% FBS, 0.4 µg/mL hydrocortisone (Sigma-Aldrich, Cat. No. H4001), 8.4 ng/mL cholera toxin (Sigma-Aldrich, Cat. No. C8052), 5 µg/mL insulin (Sigma-Aldrich, Cat. No. I5500), 24 µg/mL adenine (Sigma-Aldrich, Cat. No. A2786), and 10 ng/mL epidermal growth factor (EGF; R&D Systems, Cat. No. 236-EG). Media was removed from the dermal equivalents and the 50 µl of keratinocyte cell suspension was added to the top of each raft. The rafts were placed in the incubator for 2 hours, allowing the keratinocytes to adhere. Afterwards, 500 µl of the 50/50 EpiLife/NIKS Complete media was added to each raft, and incubated for two days. This protocol typically calls for the use of NIKS Complete medium, however, we decided to partially supplement with EpiLife medium. This is because EpiLife contains IGF-I which is the major mediator for dermal invasion from permissive keratinocytes

(Pickard *et al*., 2015). Therefore, we hypothesized that the presence of IGF-I during this growth phase may facilitate dermal invasion, if the keratinocytes were isolated from a high-grade or cancer lesion.

After incubating the submerged keratinocytes on the dermal equivalents for two days, the media was removed and rafts were lifted to an air-liquid interface. A micro spoon was used to transfer the rafts from the 48-well plate onto Millicell 30 mm, 0.4 μm inserts (Millipore, Cat. No. PICMORG50) placed in 6-well plates, where 1.1 ml of FAD media was added around each insert, at one insert per well. FAD medium consists of NIKS Complete medium without EGF, and with the addition of Ca^{++} to 1.88 mM, which facilitates differentiation of keratinocytes. The FAD media was replaced every 2 days, where residual media that accumulated around the rafts on top of well-insert membrane was removed. After 14 days, rafts were fixed overnight in 10% buffered formalin (Fisher Scientific, Cat. No. SF100-4). The rafts were subsequently washed once and stored in 70% denatured ethanol (Fisher Scientific, Cat. No. HC11001GL). Formalin-fixed rafts were then sent to Pathology Services at TBRHSC for paraffin-embedding, and preparation of 4 μm thick H&E slides.

When troubleshooting patient-raft cultures that had minimal stratification, we decided to utilize EpiLife media as the basal component to the differentiation media. We hypothesized that cultures were acclimated to the rich formula and possessed reduced proliferation when switched to FAD media. Therefore, in a subsequent trial we supplemented EpiLife with 10 ng/ml EGF, 8.4 ng/ml cholera toxin, and 2.5% FBS to simulate NIKS medium when seeding keratinocytes onto dermal equivalents (termed EpiLife-NIKS). After lifting raft cultures, we used an FAD-style supplemented EpiLife

33

medium for differentiation, whereby Ca^{++} was added to a final concentration of 1.88 mM, with 2.5% FBS and 8.4 ng/ml cholera toxin (termed EpiLife-FAD). Note that we did not further supplement EpiLife with hydrocortisone or adenine, as these are already present in HKGS-supplemented EpiLife, nor did we add insulin as HKGS contains IGF-I in place of insulin. We compared the use of NIKS medium and EpiLife-NIKS, and changed the media to FAD and EpiLife-FAD, respectively, after lifting rafts. We also tested whether wetting the raft during media changes would affect the stratification, as this is recommended in some commercial protocols. Each condition was replicated in triplicate for comparison.

2.2.7 Microscopy

Cells were visualized using an Axiovert 200 Inverted Microscope manufactured in Germany, with HBO 50 Watt AC-L2 mercury bulb connected to a MBQ 52 AC power supply. Images were taken using a QICAM 12-bit FAST 1394 camera. All phase-contrast images were taken at 200X magnification. For *mycoplasma* testing, a 350 nm blue emission filter was used.

Histology images were taken using a Zeiss Axioskop 50 manufactured in Germany, with QImaging Retiga 1300 camera. All histology images were taken at 100X magnification.

3. Results

3.1 Results from E6 knock-down on downstream processes

3.1.1 Expression levels of E7 and hTERT

In previous work, cultures of CaSki and SiHa were transfected in T-25 flasks as described, and both Western blot and RT-qPCR analysis was performed (**Figure 4**). We sought to utilize these same cDNA samples to analyze downstream effects of E6 knock-down. Analysis of E7 expression revealed a large variability in CaSki cells as compared to SiHa cells. There was no change in E7 expression for CaSki cells, as the average fold change was close to 1 for all Rosetta and Scrambled treatments (**Figure 8**). SiHa cells showed markedly decreased expression of E7 for most treatments regardless of DsiRNA type. Expression of hTERT was also more variable for CaSki than SiHa cells. The expression of hTERT was not significantly different between Rosetta and Scrambled controls for any treatment in CaSki or SiHa.
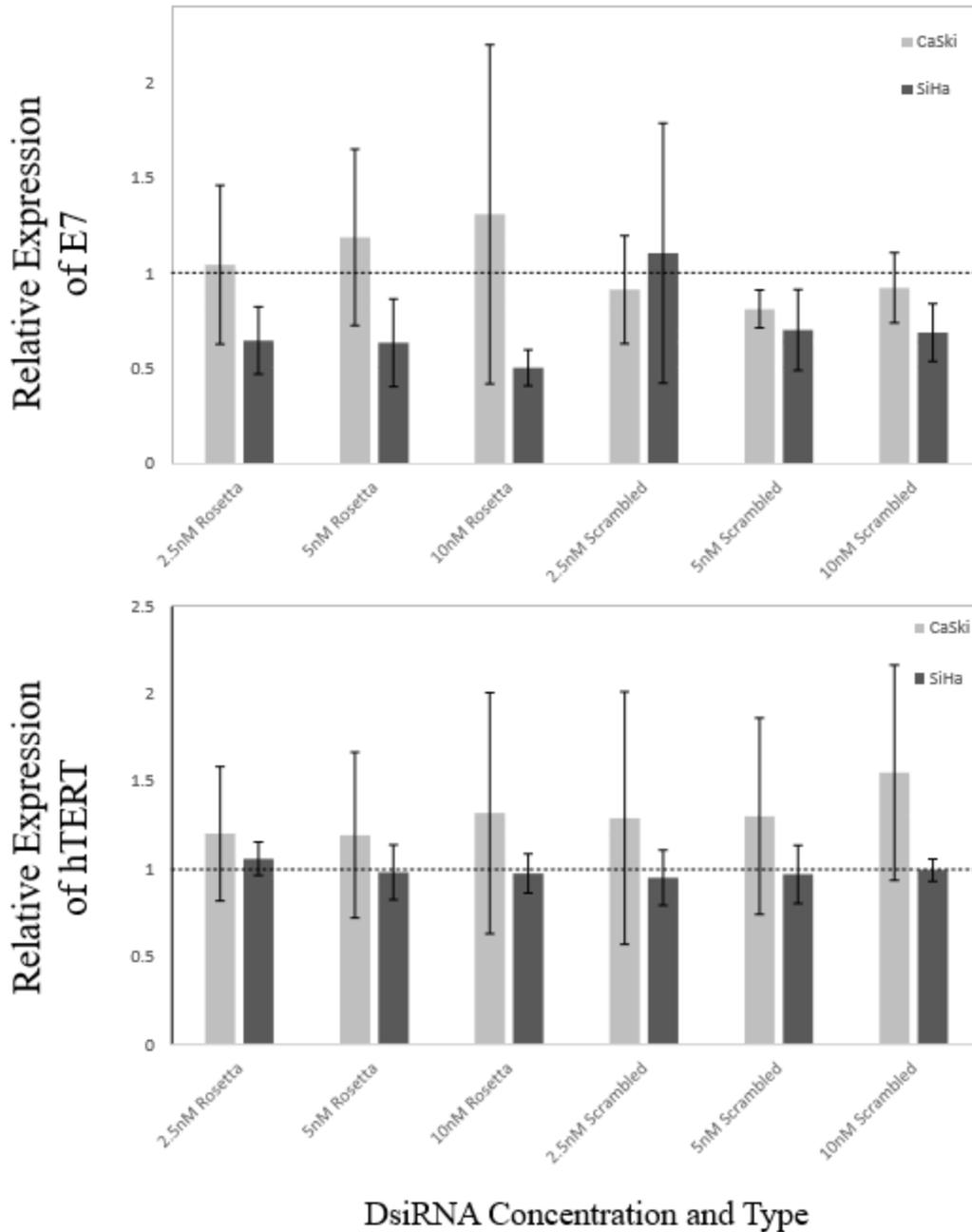
Figure 8. Relative expression of E7 and hTERT 48 hours after E6 knock-down. Expression levels were determined relative to HPRT-1. Treatments were normalized to the media-only control, where a fold-change of '1' indicates no change. No significant difference was found between Rosetta and Scrambled DsiRNA treatment. Data represents the mean ± SD (n=4).

3.1.2 Validation of C9/11 control DsiRNA

For further downstream analysis, we intended to replace the Scrambled DsiRNA control with the C9/11 DsiRNA control. By doing so, off-target effects of the Rosetta DsiRNA oligonucleotide can be maintained, while E6 knock-down is abolished. Cultures were treated with the C9/11 DsiRNA as described, and RT-qPCR analysis indicated no significant difference in E6 fold-change relative to media-only condition (**Figure 9**). Levels of E6 expression were higher than the media-only condition for all C9/11 treatments in both CaSki and SiHa cells, although this was not significant. Therefore, we continued to utilize the C9/11 DsiRNA control when using Rosetta DsiRNA for E6 knock-down.
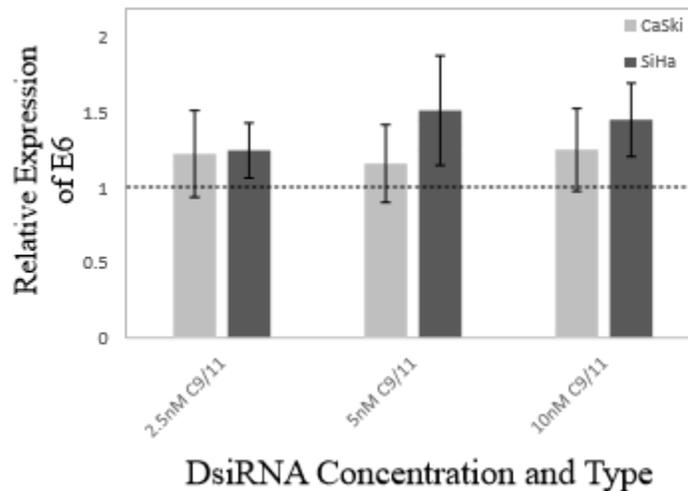
Figure 9. Relative expression of E6 48 hours after treatment with C9/11 DsiRNA. Expression levels were determined relative to HPRT-1. Treatments were normalized to the media-only control. No significant difference was found between C9/11 and media-only controls. Data represents the mean ± SD (n=4).

3.1.3 Analysis of p21$^{WAF1/CIP1}$ expression

Previous Western blot data has demonstrated a recovery in p53 levels upon E6 knock-down, though this data was not statistically significant. The expression levels of p21$^{WAF1/CIP1}$ were quantified to support whether the restored p53 was transcriptionally active. Levels of p21$^{WAF1/CIP1}$ were detected but not quantifiable in SiHa cells (data not shown). Data from the CaSki cells revealed no significant increase in p21$^{WAF1/CIP1}$, nor any general trend (**Figure 10**).
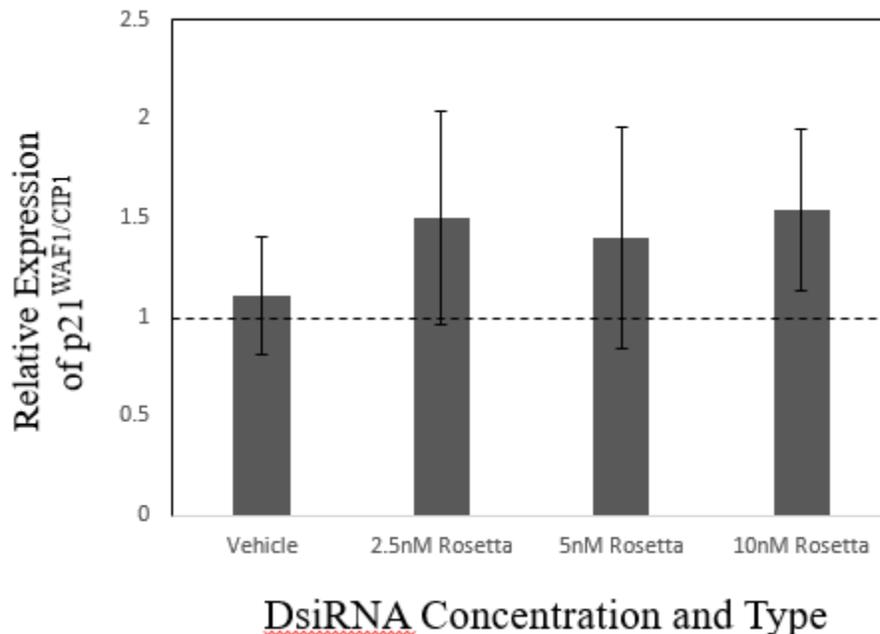
Figure 10. Expression of p21$^{WAF1/CIP1}$ in CaSki cells following E6 knock-down. Expression levels were determined relative to HPRT-1. Treatments were normalized to the media-only control. Previous work had demonstrated variable and non-significant p53 restoration upon E6 knock-down. The levels of p21$^{WAF1/CIP1}$ were undetectable in SiHa cells. Data represents the mean ± SD (n=3).

3.1.4 MTT viability assay following E6 knock-down

MTT assays were performed on transfected cultures of CaSki and SiHa cells to assess changes in viability. In this respect, decreases in cell growth and/or increases in cell

death can be inferred from overall changes in viability. There was no significant difference between Rosetta DsiRNA treatment versus the C9/11 control (**Figure 11**).
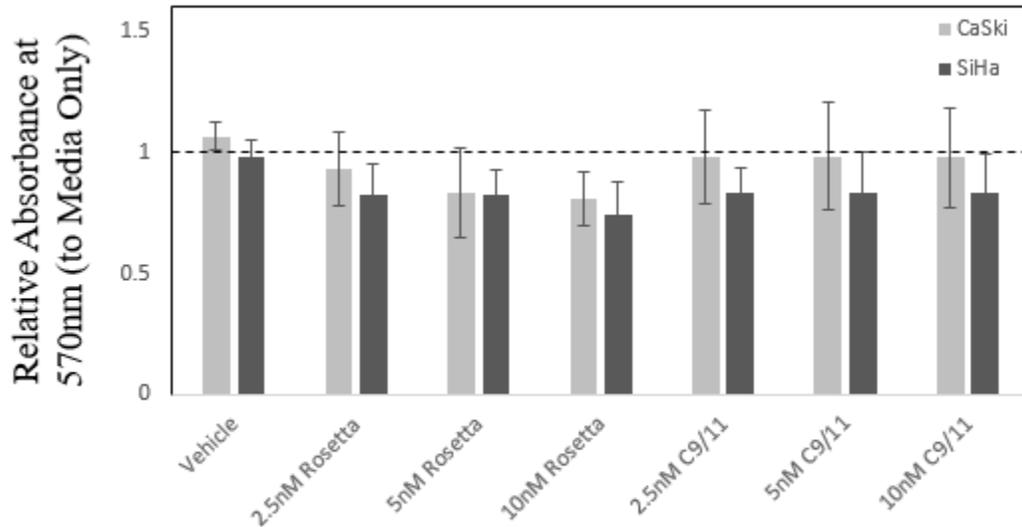
Figure 11. **MTT viability assay of CaSki and SiHa cells transfected with DsiRNA.** Cultures were seeded into 24-well plates and transfected with either Rosetta DsiRNA or C9/11 DsiRNA. The colorimetric assay was performed 48 hours later and absorbance was measured at 570 nm subtracting the background at 650 nm. There was no significant difference between Rosetta and DsiRNA treatment. Data represents the mean ± SD (n=4).

3.1.5 Cell-cycle and apoptosis assays

Although no significant changes in cell viability were detected by the MTT assay, we sought to perform more sensitive experiments to assess apoptotic events and possible changes in cell-cycle. Additionally, we assessed cultures at both 48 and 96 hours after transfection. Transfected cultures were split equally between apoptosis assays and cell-cycle analysis. Full cell-cycle results are shown in **Figures A3** and **A4**. There were no significant differences between Rosetta and C9/11 treatments. In a subsequent analysis, a G1:S ratio was calculated to suggest whether or not cells were slowly accumulating in an

arrested state. A significant difference (P<0.05) was found between Rosetta DsiRNA and

C9/11 control for CaSki 48 hours after treatment (**Figure 12**).
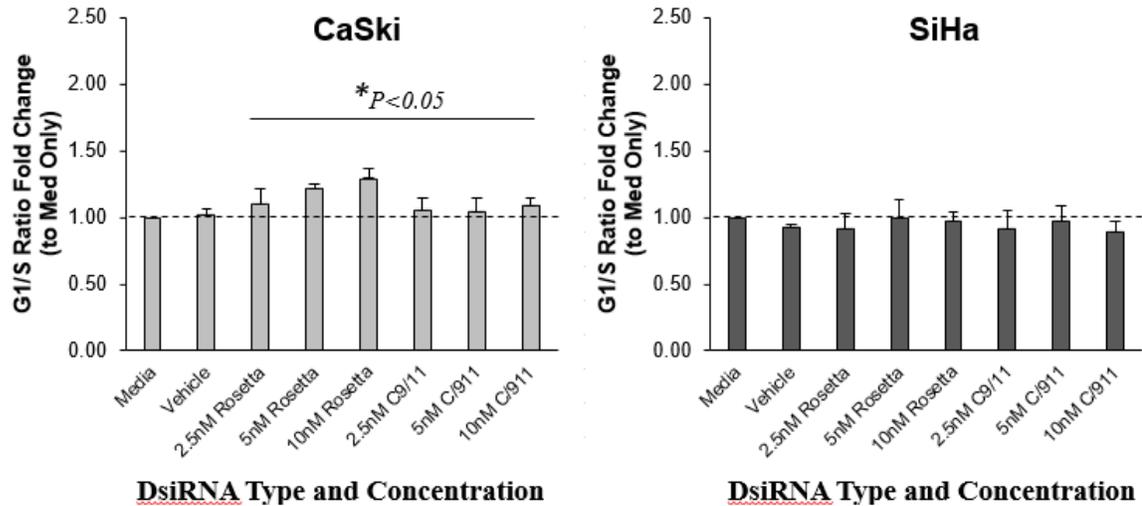
Figure 12. G1:S ratio of CaSki and SiHa cells 48 hours after treatment with DsiRNA.
The ratio of cell populations in the G1 phase versus S phase show a statistical difference
between Rosetta and Control DsiRNA ($P<0.05$) at 5 nM and 10 nM Rosetta DsiRNA for
CaSki. No statistical difference was found for CaSki at 96 hours, or SiHa at 48 and 96
hours (data not shown). Data represents the mean ± SD (n=3).

When assessing apoptotic events, there were no significant differences between

Rosetta and C9/11 DsiRNA treatments for early, late, and total apoptotic events, at 48 or

96 hours, for either cell type. Data are illustrated in **Figures A5-A8**.

3.1.6 Cell growth analysis

To assess changes in cell growth over a longer period, we transfected cultures

periodically over several passages to observe changes in proliferation. This longer time

interval can illustrate more minute changes that the previous assays cannot. This

experiment was done in a single replicate (**Figure 13**). The growth curve suggests that the

cells respond negatively to DsiRNA treatment, regardless of whether it was Rosetta or the

C9/11 control.
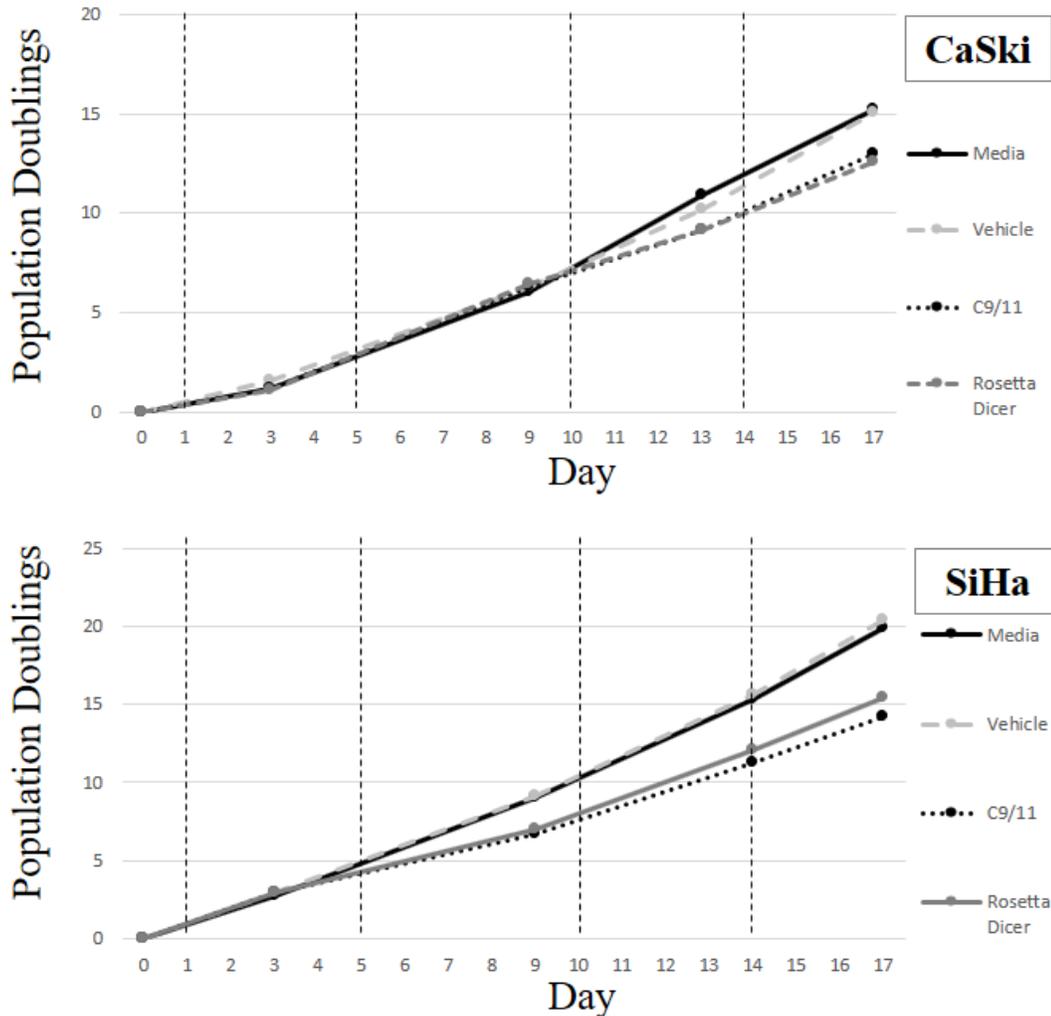
Figure 13. Growth curve of CaSki and SiHa cells transfected periodically with DsiRNA. Cultures were transfected 24 hours after passaging. Transfection days are illustrated by a vertical dotted line. Cultures were transfected with 10 nM of Rosetta DsiRNA or C9/11 control (n=1).

3.2 Results from creating patient-derived cervical keratinocyte cell cultures

3.2.1 Phase I - methods for isolating and propagating cervical keratinocytes

Thirty biopsy specimens were acquired over a 7-month interval, from August 2016 to March 2017. The Stanley (2002) method was used on the first 5 biopsies to validate our ability to process biopsy specimens. These samples however, yielded only sparse fibroblast

colonies. The modified Liu *et al.* (2016) method was used on the other 25 biopsy specimens. Initially, when colonies were established 4 or 5 days after biopsy processing, the media was switched to KGM containing 0.5% FBS. This resulted in significant fibroblast growth by the second or third week (**Figure 14**). Upon passaging one of these cultures, the cells adhered and slowly lifted over the course of 5 days, where the presence of serum was suspected to be a factor. Therefore, there were a total of 6 biopsies between the Stanley method and presence of serum for which a culture lifespan could not be determined. Of the remaining 24 biopsies acquired, the media was switched to serum-free KGM, instead of KGM-0.5% FBS, once the cell colonies were established following biopsy processing. Some of these cultures differentiated before passaging (n=4), whereas others were successfully passaged and continued to grow before differentiating (n=3). When using serum-free KGM, there were no further instances of keratinocytes lifting from the culture flasks, nor was there sustained fibroblast growth.
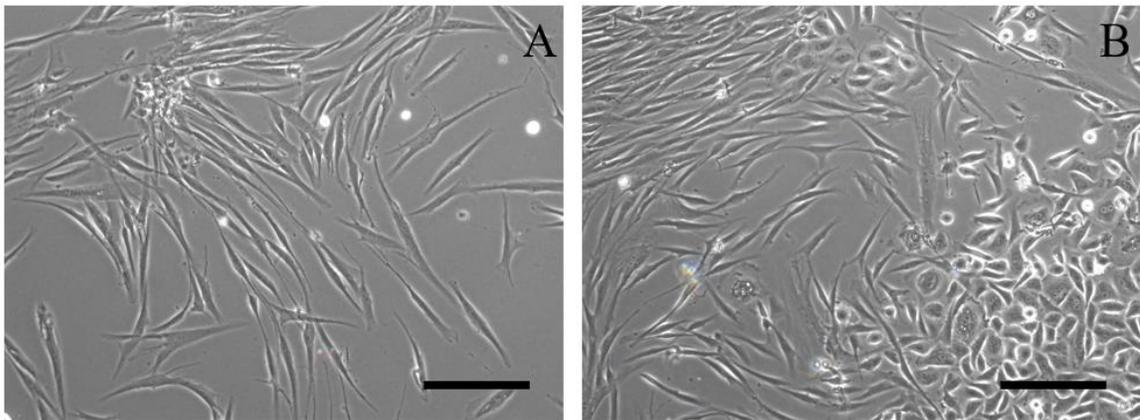
**Figure 14. Fibroblast contamination from cultures containing 0.5% fetal bovine serum in Keratinocyte Growth Medium.** Fibroblast colony present at Day 15 in patient culture #44 (**A**). Fibroblast growth present near a proliferating keratinocyte colony at Day 21 in patient culture #13 (**B**). Fibroblasts were identified by morphology. Scale bars represent 200 microns.

Biopsy specimens varied considerably in size. The smallest specimens (6/25) were approximately 1 mm in all dimensions, and were too small to be minced with the curved iris scissors. The largest specimens (8/25) were roughly a uniform 4 mm across. Most of the specimens (11/25) were between these sizes, and were typically 2-3 mm wide and ~1-2 mm in height and depth. This likely reflects the bite of the Tischler Morgan 3 mm x 7 mm biopsy forceps, where the size varied by the ability of the physician to precisely sample the lesion. In turn, the smallest biopsy specimens would be from the very edge of a lesion (as the first and better biopsy taken was used for standard-of-care). There were notable differences in the ability to establish proliferative cultures from the various biopsy sizes (**Table 2**). The ability to establish cultures from biopsy specimens correlated with size.

Table 2. Successful establishment of keratinocyte cultures from cervical biopsies. Larger biopsy specimens had a higher probability of producing proliferative cultures. Note that of 30 specimens acquired, 5 were used with the Stanley (2002) method and are not included in this chart. Nearly half of all specimens that yielded colonies did not proliferate (6 out of 14 total). Small biopsies typically represent those that were 1 mm x 1 mm x 2 mm or smaller, whereas large biopsies were uniform 3-4 mm specimens, and medium biopsies lie in between these dimensions, typically at half the size of a large biopsy.

Relative biopsy size	Number of biopsies	Number yielding colonies with no growth	Number yielding colonies with sustained growth	Probability of growth
Small	6	2	0	0%
Medium	11	4	2	18%
Large	8	0	6	75%

Differentiation was evident upon microscopic examination, as cultures would exhibit noticeably reduced growth (i.e. modest changes in confluency over the course of one week). Cells would then cease to proliferate and markedly increase in cross-sectional

area for approximately one or two more weeks (**Figure 15**). Therefore, lifespan was estimated retrospectively from the dates by which cells dramatically increased in size and had previously shown decreased proliferation. The median time to differentiation was 4 weeks. Culture lifespan from actively proliferating cultures is depicted in **Figure 16**. A slight heterogeneity existed between proliferating and differentiated cultures between patients, as exemplified in **Figure 17**. Mainly, cultures may differentiate at varying sizes, though they still exhibited uniformly flattened keratinocytes with centred nuclei.
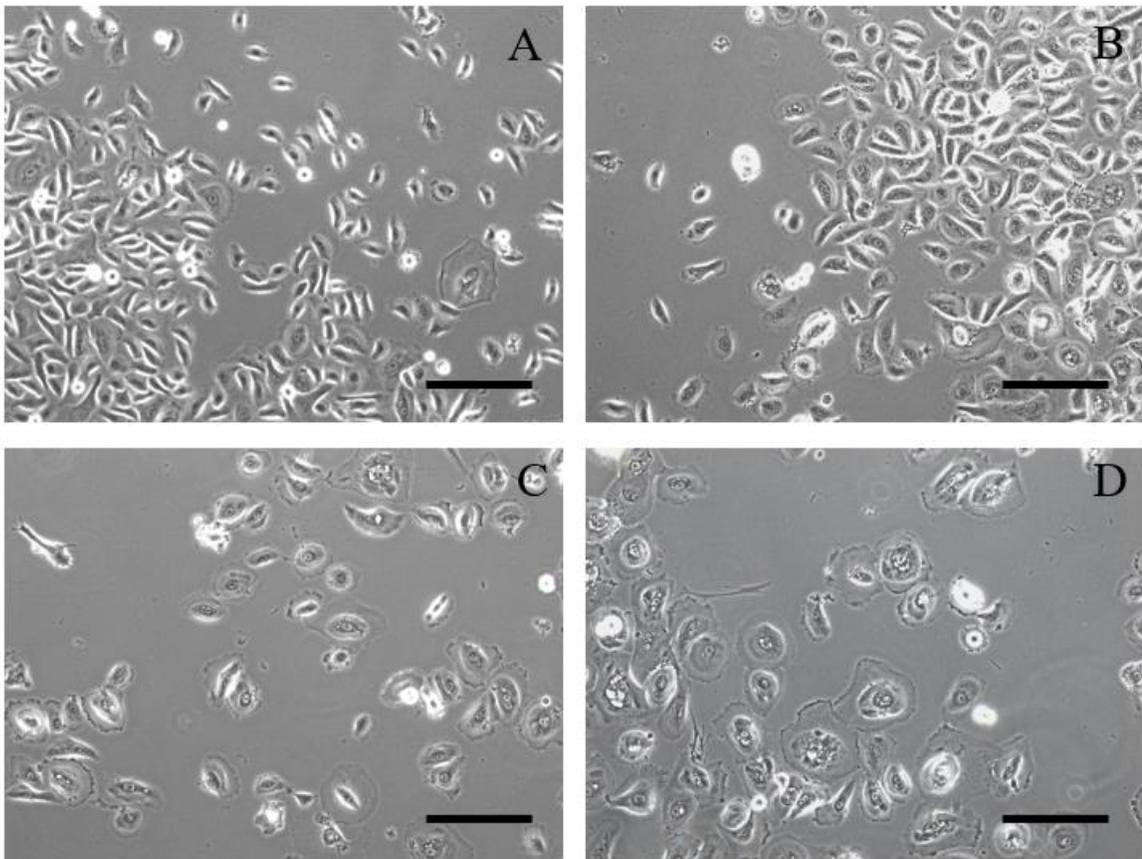
Figure 15. Visible and progressive differentiation of keratinocytes from patient isolate #22. Keratinocytes are visibly proliferating up to Day 21 (**A**). Keratinocytes have modestly but homogeneously increased in their apparent size by Day 26 (**B**). Keratinocytes are no longer proliferating, cell nuclei become centred, and cell membrane begins to spread along the flask evenly around the cell by Day 34 (**C**). Cells have uniformly increased in size by Day 40 (**D**). Scale bars represent 200 microns.
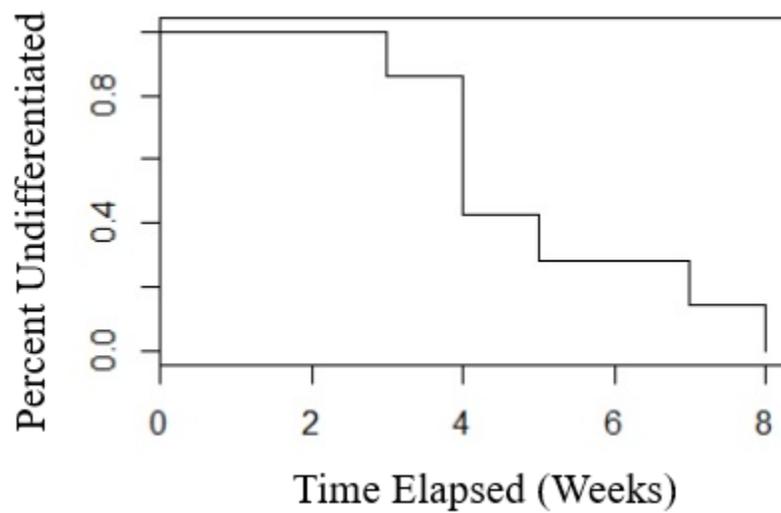
Figure 16. Differentiation plot of keratinocytes grown from cervical biopsy specimens *in vitro***.** Cultures were established from 7 of 24 biopsy specimens. The median proliferating culture established would differentiate by the fourth week. Image was generated in R version 3.2.2.
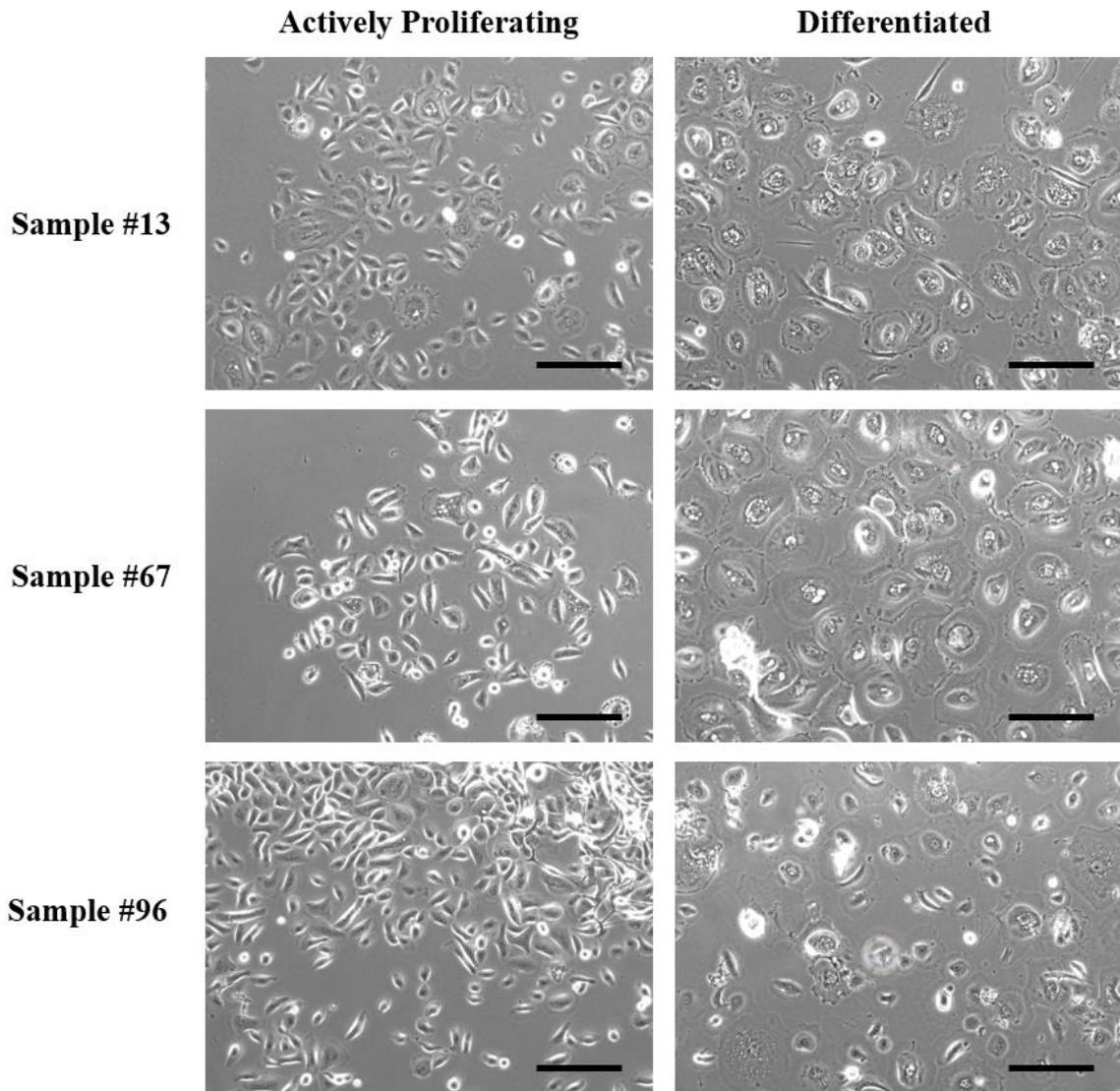
Figure 17. Modest variations between patients in phenotype of proliferating and differentiated keratinocytes. Cultures from patients #13 and #67 appear very similar in morphology between their respective proliferating and differentiated cultures. Proliferating keratinocytes in culture #96 appear normal, however the differentiated keratinocytes appear heterogenous in their apparent size. Scale bar represents 200 microns.

Although the doubling time could not be accurately measured for most cultures, the approximate rate-of-change in confluency between cultures seemed to be similar, with an approximate doubling time between 2 and 3 days. This metric however, does not reflect the total number of cells that initiated the culture, and therefore does not reflect the total yield of cells acquired *in vitro*. A summary of biopsy metrics and final flask size is summarized in **Table 3**. Under these conditions, culture lifespan was the largest contributor to cell yield. Images of representative biopsy sizes are shown in **Figure 18**.

Table 3. Summary of biopsy specimen metrics on size, lifespan, and total relative cell yield. Cultures were progressively scaled from T-12.5 flasks, to T-25 flasks, and subsequently T-75 flasks where they were maintained. Median culture lifespan was 4 weeks.

Patient Number	Biopsy Size	Culture Lifespan (Weeks)	Order of Flask Size at Differentiation
13	Large	4	T-25
17	Large	4	T-12.5
22	Medium	4	T-25
28	Medium	8	T-75*
59	Large	3	T-12.5
67	Large	5	T-25
96	Large	7	T-75*

*Cultures were passaged once from the first T-75 flask but differentiated shortly thereafter, not substantially altering the total cell yield from the first T-75.
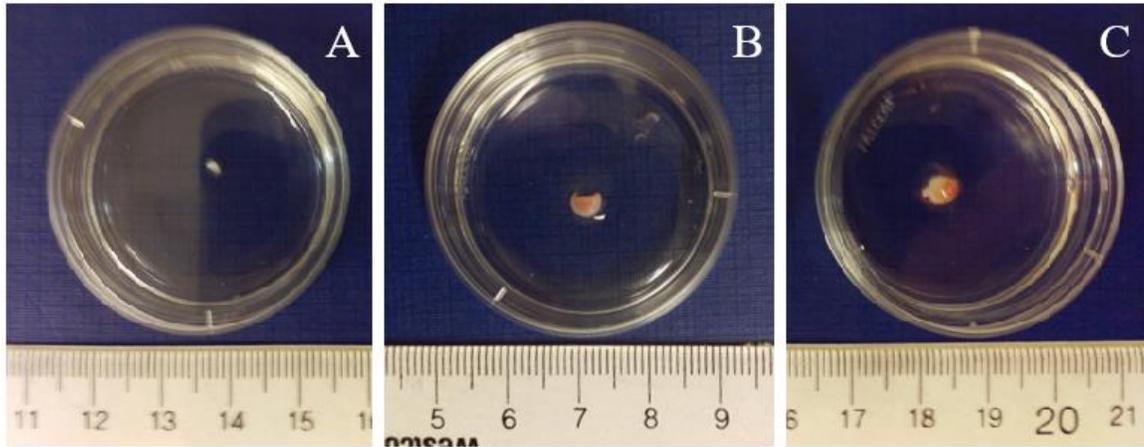
Figure 18. Images of biopsy specimens illustrating variations in size. Sizes of specimens differed markedly between patients, from small specimens ~ 1 mm x 1 mm x 1 mm (**A**), medium specimens ~ 2 mm x 2 mm x 3 mm (**B**), and large specimens ~ 3 mm x 3mm x 3mm (**C**).

3.2.2 Phase II – increasing in vitro lifespan of cultures and organotypic raft construction

The cell culture media was switched from KGM to EpiLife media containing Human Keratinocyte Growth Supplement, as this formulation is rated to produce over twice as many population doublings (Li S *et al*., Cascade Biologics Inc). This increase in lifespan is attributed to the decreased Ca^{++} concentration, the presence of IGF-I instead of insulin, and an increase in the number organic components and inorganic salts. In addition, once cultures had been established from processed biopsies in the presence of 5% FBS, the media was switched to serum-free fully-supplemented EpiLife containing the ROCK inhibitor Y-27632, which inhibits differentiation of epithelial cells, increasing lifespan and potentially promoting immortalization (see 'Materials and Methods').

Additional patient information was collected for the second phase of this study. Patients had their cervix swabbed for HPV typing, and their age and lesion grade was recorded. From the first phase of the study, it was also observed that some biopsy specimens would digest well with collagenase – where minced tissue fragments would digest into a visibly turbid cell suspension, and residual extracellular matrix would expand

and clump – while others would not digest at all with collagenase. This observation appeared to be correlated with establishing colonies and therefore, in the second phase it was noted whether each biopsy digested well or poorly as an additional parameter. Overall observations and results for establishing cultures are illustrated in **Table 4**. Interestingly, under these modified culture conditions, all instances where colonies were established from specimens yielded sustained cell growth. Cultures were established from 6 of 14 biopsy specimens (~43% efficiency). The average specimen in Phase II was also notably smaller than those in Phase I of this study. As biopsy size was correlated with efficiency in Phase I, this observation may suggest that our overall efficiency in establishing a proliferating culture was markedly improved by these new culture conditions.

There were two patient cultures that survived long enough to test cryogenic storage and have their doubling times accurately calculated via cell counts when passaging cultures. Cultures 3UI and AV6 both survived storage in liquid nitrogen with high re-adherence rates. Culture 3UI possessed a doubling time of ~30 hours, and culture AV6 possessed a doubling time of ~24 hours. The median culture lifespan in the second phase of this study was 4.5 weeks. Therefore, our modifications to the cell culture media have effectively reduced doubling time without significantly altering temporal *in vitro* lifespan.

Table 4. Summary of biopsy parameters, patient information, and culture growth. Biopsy size and visible digestion were noted on the day of sample processing. Patient's age, HPV type(s), and lesion grade were recorded. Culture lifespan was measured as previous, to time of differentiation. Cultures were established in T-12.5 flasks and scaled up T-25 flasks, then to T-75 flasks before consecutive passaging in T-75 flasks, were each passage seeded at 10% confluence. Median *in vitro* lifespan was 4.5 weeks.

Sample Identifier	Biopsy Size	Digestion	Patient Age (Years)	HPV Type(s)	Lesion Grade	Lifespan (weeks) / Flask Scaling & Passage
M33	Medium	Poor	56	39	*	-
UB1	Small	Poor	27	45,59	I	-
8N8	Small	Poor	24	16	III	-
QA7	Small	Poor	35	45	Neg.	-
A1U	Large	Good	25	6	I	5 / T-75 (P2)
LY2	Medium	Poor	23	53,66	I	-
HL7	Medium	Poor	29	45	III	-
IW9	Small	Good	32	16	II-III	5 / T-75 (P2)
78I	Small	Poor	22	52,82,89	Neg.	4 / T-25
V7V	Small	Poor	69	16,90	Neg.	-
3UI	Medium	Good	36	31,45,89	II	6 / T-75 (P7)
04P	Medium	Good	23	51,54,81	I	4 / T-25
R41	Small	Poor	54	58	Neg.	-
AV6	Medium	Good	27	16	II	4 / T-75 (P6)

*Patient presented with metaplasia

When assessing the parameters of successfully established cultures, several trends emerge. Firstly, most patients are in their mid-twenties to mid-thirties, which is a narrow range for identifying correlations with age. Secondly, there was no obvious correlation with lesion grade or the presence of high-risk HPV types in an established culture: only 1 of 3

CIN III lesions were successfully cultured, and only 3 of 8 specimens that contained high-risk HPVs (i.e. 16, 18, 31, and/or 45) were successfully cultured; while 2 of 4 CIN I lesions, and 1 of 4 CIN negative lesions were successfully cultured. The two cultures that were passaged the longest were isolated from CIN II lesions, suggesting that lesion grade also does not predict *in vitro* proliferative capacity. These parameters however, may be masked by the importance of biopsy size, or other parameters. Only 2 of 7 small biopsies yielded cultures, while 3 of 6 medium and 1 of 1 large biopsies yielded cultures. The first phase of this study, which showed biopsy size was the biggest correlate; had fewer small biopsies. Lastly, tissue digestion and visible turbidity appeared to be strongest correlate in 'Phase II', where 5 of 5 well-digested biopsies yielded cultures, and only 1 of 9 poorly digested samples yielded a proliferating culture.

For all proliferating cultures, we intended to generate organotypic raft cultures in triplicate as soon as reasonably possible, given that we did not know when cultures would reach their lifespan, or whether they would survive cryogenic storage in liquid nitrogen. This meant generating rafts from near-confluent T-25 flasks, or sufficiently confluent T-75 flasks. All of these cultures were tested for *Mycoplasma* indirectly using the J2 fibroblast cell line as an indicator. All cultures tested negative for *Mycoplasma* under these parameters (**Figure 19**).
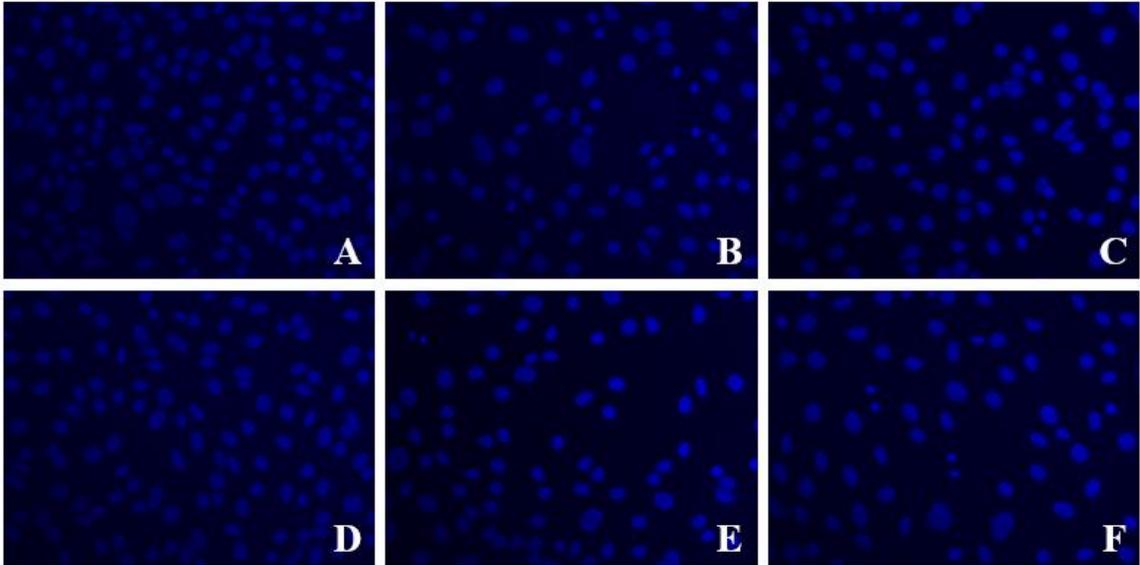
Figure 19. Fluorescent images of DAPI-stained J2 fibroblasts treated with conditioned media from patient-derived keratinocyte cultures. Fibroblasts were grown in the presence of conditioned media for 3 days. Images showing samples 3UI (**A**), 04P (**B**), 78I (**C**), A1U (**D**), IW9 (**E**), and Untreated J2 fibroblasts (**F**). Images taken at 200X magnification.

When seeding keratinocytes onto dermal equivalents, the relative size of the keratinocytes was noted from the TC-10^{TM} Cell Counter. Typically, keratinocytes from patients or commercial sources were homogeneously between 16 and 18 µm in diameter while actively proliferating. When cells were beginning to differentiate, a discrete proportion of the population would exist between 22 to 24 µm. For example, when 30-50% of the cells were 22-24 µm, the culture would differentiate on the current passage when re-seeded. This observation held true for all cultures in the second phase. The proportion of small-to-large cells was recorded upon passaging to note when cultures would differentiate. At the time of raft culture, it was noted for patient cultures A1U, IW9, and 78I, that one-third of the population existed at 22-24 µm, and 04P was one-half 22-24 µm; illustrating that these cultures were near their *in vitro* lifespan at the time they were seeded onto dermal equivalents. Indeed, the remaining cell suspension (i.e. in excess from seeding for raft

cultures) were re-seeded back into monolayer culture, and differentiated without further passaging. Culture 3UI was the only sample that was homogeneously small (i.e. 16-18 μm) at the time of 3D culturing.

Raft cultures were created in technical triplicates when keratinocyte numbers permitted (i.e. A1U, 04P, 3UI, IW9) and duplicate when cell numbers were limiting (i.e. 78I). We proceeded with raft culturing as described (see '*2.2.6 Construction of organotypic raft cultures*'), and cultures were maintained at the air-liquid interface for 14 days. Raft cultures were then formalin-fixed and sent to Pathology Services at TBRHSC for paraffin-embedding, slide preparation, and H&E staining. The resulting representative H&E images are illustrated in **Figure 20**. From the representative images, it appeared that much of the epidermis was sloughed off during processing. Similarly, as all of the samples – other than 3UI – grew rather poorly, it seems these 3D cultures were significantly affected by the fact that the keratinocytes had nearly reached their *in vitro* lifespan. Interestingly, although IW9 did not yield much epidermis, regions that were akin to epithelial invasion of the dermis were visible in all technical replicates (**Figure 21**). These events were not evident in any of the other organotypic raft cultures.
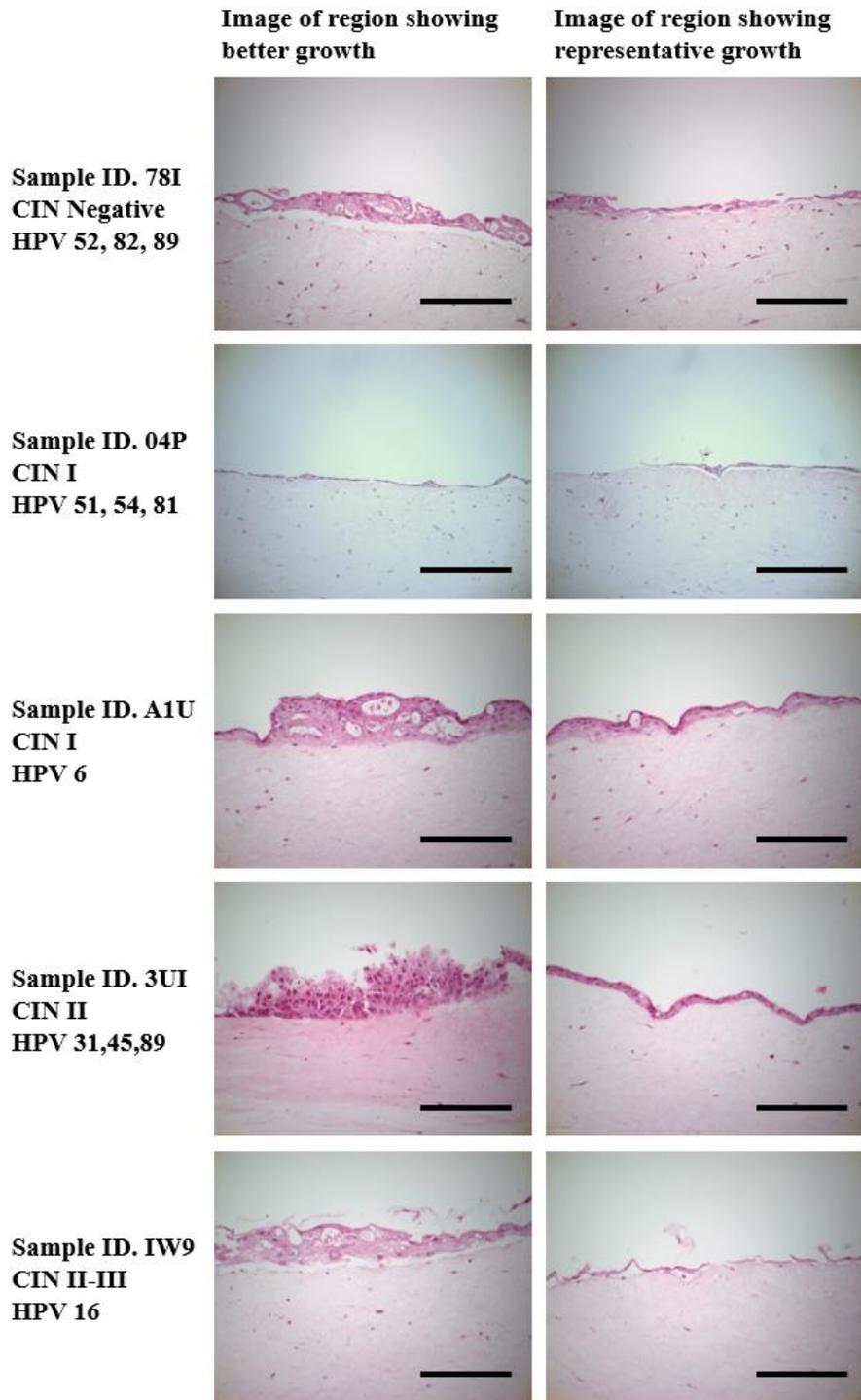
Figure 20. H&E images of organotypic raft cultures grown using patient-derived cervical keratinocytes. Dermal equivalents were prepared with type-IV rat tail collagen and human neonatal foreskin fibroblasts. After 24 hours, keratinocytes were seeded on top and incubated for 2 days. The rafts cultures were then lifted and cultured at air-liquid interface for 14 days before formalin fixation. Formalin-fixed raft cultures were paraffin-embedded and 4 μm sections were prepared for H&E staining. Stained sections did not visibly differ between technical replicates. Scale bars represent 200 microns.
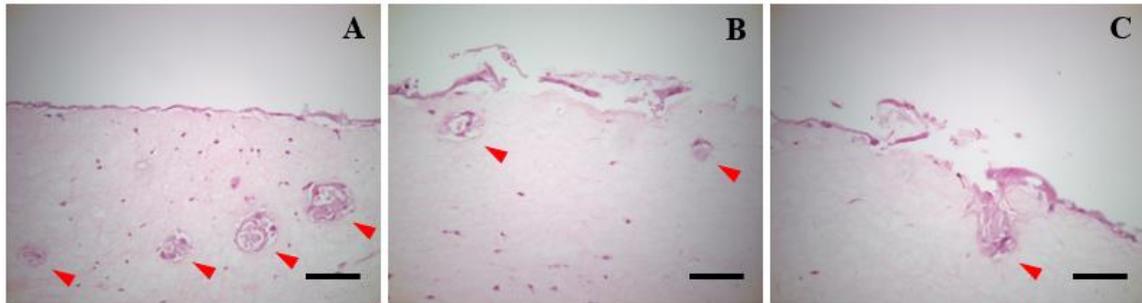
Figure 21. Organotypic raft culture using IW9 keratinocytes showing possible invasion events. Keratinocyte culture IW9 is derived from a CIN II-III lesion that tested positive for HPV 16. Possible instances of keratinocyte invasion of the dermis are indicated by red arrows. This possible invasion was evident in all technical replicates (**A**, **B**, and **C**). Scale bars represent 100 microns.

Given that 3UI appeared to be the most successful 3D culture, even though it still experienced significant dermal detachment and poor keratinocyte growth around most of the raft, we questioned whether altering the media formulation or rafting conditions could improve epithelial growth. As EpiLife is a richer medium than FAD, we reasoned that keratinocytes may have a reduced growth rate when switched to FAD medium. Therefore, EpiLife media was prepared with the differentiation components of FAD media, in the hope that this richer formulation would sustain keratinocyte growth. Additionally, some protocols call for 'raft-wetting' where the rafts are periodically wet with media to simulate the wetting of the mucosa. Twelve rafts were prepared using 3UI: six with FAD media and six with EpiLife-Differentiation media, 3 with wetting and 3 without wetting for each media. All four conditions yielded similar results (**Figure 22**), with limited epithelial growth. Notably, these rafts yielded less epithelial growth than previously created rafts. The cells used in this trial were of two passages higher and had been retrieved from cryogenic storage which may have affected the results.
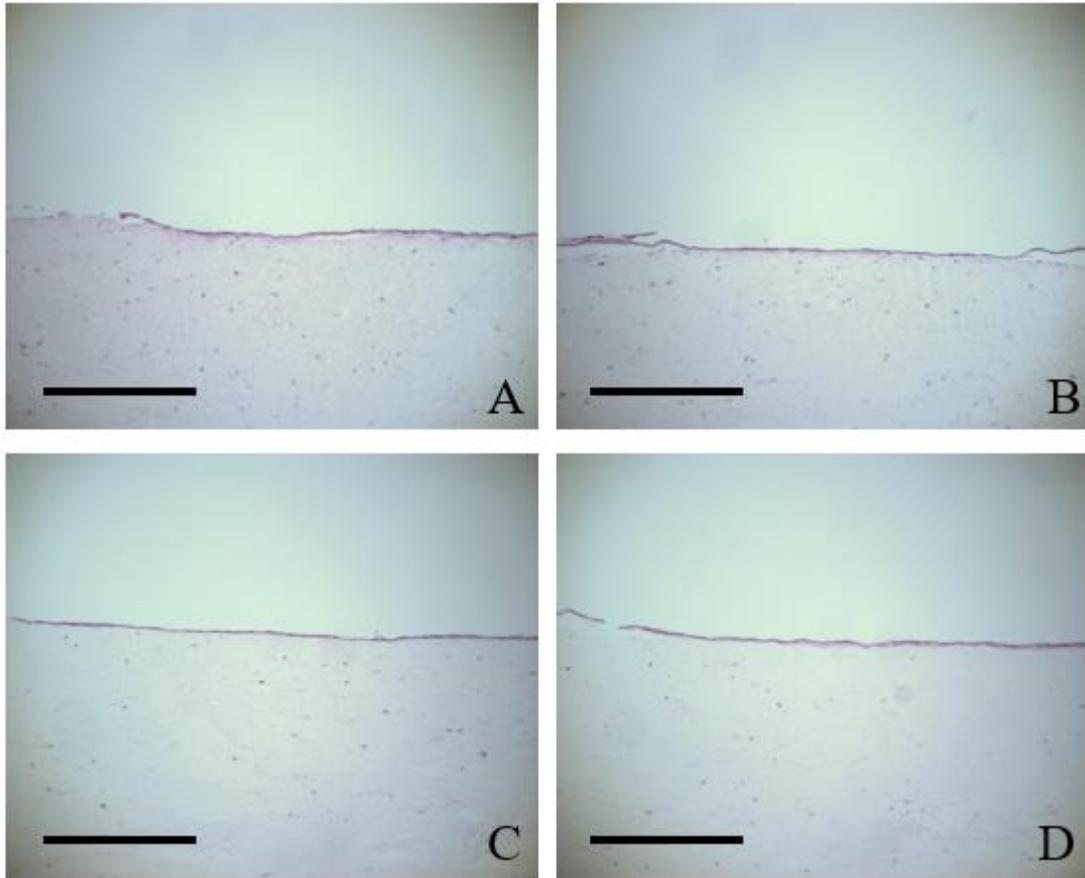
Figure 22. H&E images of organotypic raft cultures of 3UI. Organotypic rafts were created in triplicate using FAD media with (**A**) and without wetting (**B**) rafts with media, as well as EpiLife formulated to simulate FAD with (**C**) and without (**D**) wetting. Scale bar represents 200 microns.

4. Discussion

4.1 Downstream effects of E6 knock-down

In this study, we found minimal downstream effects resulting from E6 knock-down on the cell lines CaSki and SiHa, even though our level of knock-down similar to literature (Jiang and Milner, 2002; Leitz *et al*., 2014; Khairuddin *et al*., 2014). Given that p53 restoration had been shown to be quite variable, it is unsurprising that p21$^{WAF1/CIP1}$ levels are unrestored, or that there are no measurable changes in apoptosis.

Importantly, targeting the E6 splice site with RNAi seemed to preserve E7

expression as hoped, substantiating the rational design of this oligonucleotide. Interestingly, even though E6 levels were measurably decreased, there was no reduction in hTERT levels. It may be that hTERT levels would decrease at a different time point, or that only low levels of E6 are required to saturate hTERT transcription.

It is unclear why these cell lines seem to respond poorly to RNAi. It may be that these cell lines have adapted to their *in vitro* culture conditions since their founding (Friedl *et al*., 1970; Pattillo *et al*., 1977), perhaps undergoing epigenetic or karyotypic changes that have selected for quickly diving cells *in vitro*. For these reasons, there are significant merits to developing new patient-derived cell lines.

4.2 Processing biopsy specimens

In this study, we utilized a slightly modified version of the Liu *et al*. (2016) method to process biopsy specimens. Briefly, after coating tissue culture flasks with type I collagen, we added pure FBS to the coating in the hopes that growth factors, cell adhesion molecules, or other signalling and mitogenic factors from the serum would adhere to the collagen-coating, and thus the tissue culture flask. These factors in turn, would help mediate the adaptation of cells to monolayer culture, after being liberated from biopsy specimens. In Liu *et al*. (2013) it was found that the presence of serum in the media greatly increased the adhesion of tissue-liberated keratinocytes to the culture flask, with or without the presence of a collagen coating. We also reasoned that since the explant methodology of Stanley (2002) minces tissue fragments and adheres them to culture flasks in pure FBS, that FBS itself may act as a flask coating and facilitate the adaptation of cells to monolayer culture. During the course of experimentation, it was noted that while most of the colonies

established from processed biopsies existed as monolayer cells, some colonies were initiated as tissue fragments fused to the culture flask (**Figure A9**). This indicates that although digestion with collagenase does liberate individual cells, it also facilitates the transfer of these 'micro' explant fragments into culture. Thus, minced biopsy specimens that are subsequently digested with collagenase should not be treated as single-cell suspensions, as this may contribute to cell losses.

One hurdle in the establishment of monolayer cultures from epithelial biopsy specimens is the significant potential for microbial contamination. The Liu *et al*. (2013) method did not indicate the number of hysterectomies acquired, nor whether any of the cultures were contaminated once cultures were established. The Liu *et al*. (2016) study however, acquired only six biopsy specimens total, and indicated no instances of contamination. For the vaginal and oral tract, the most significant sources of contamination are yeast, Gram negative bacteria, and potentially *Mycoplasma* (Stanley, 2002). Indeed, Schweinfurth *et al*. (2006) reported that bacterial overgrowth was a significant hurdle in their initial protocol to establish epithelial cell cultures from upper respiratory epithelium, though the details surrounding this contamination are not indicated. Interestingly, Rheinwald and Beckett (1981) acquired 22 biopsy specimens from the tongue and pharynx of different patients, where 7 became contaminated with yeast despite the fact that specimens were transported and rinsed with media containing amphotericin b (concentration not indicated) – the main antifungal agent used in tissue culture. Stanley (2002) recommends using amphotericin b at concentrations of 5-10 µg/ml for transport media and buffered saline washes, which was also reported as the method in Liu *et al*. (2013). We utilized amphotericin b at a concentration of 5 µg/ml in both the transport

media and DPBS washes of specimens, and experienced no instances of yeast contamination. Amphotericin b interacts with ergosterol in the membrane of fungi, forming a channel for monovalent ions. This altered membrane permeability leads to cell death, but in the presence of ideal carbon sources and sufficient nutrients, fungi – yeast in particular – can counteract the effects of lower amphotericin b concentrations (Bolard *et* al., 1993). We used 20X antibiotic/antimycotic specifically to reach the concentration of 5 μg/ml; and as this also yielded a penicillin concentration of 2,500 units/ml and a streptomycin concentration of 2.5 mg/ml, we had no instances of bacterial growth. Unfortunately, none of these publications reported the *Mycoplasma* status of established cultures. *Mycoplasma* is inherently resistant to penicillin antibiotics as they possess no peptidoglycan cell wall, but some species are susceptible to streptomycin as it binds to the 30S ribosomal subunit thereby inhibiting protein translation. We chose to add gentamicin to transport media and DPBS washes, which also interacts with the 30S ribosomal subunit, but has a more broad-spectrum activity against *Mycoplasma* than streptomycin (Taylor-Robinson and Bebear 1997), has a stronger bactericidal (as opposed to bacteriostatic) activity, and possesses a lower effective concentration than streptomycin in cell culture (Fischer, 1975). Though we did not test cultures for *Mycoplasma* in 'Phase I' of this study, we found no evidence of *Mycoplasma* contamination when testing the established keratinocyte cultures from 'Phase II'. Therefore, it would seem our antimicrobial cocktails and experimental protocols have avoided contamination issues that were present in many other studies.

4.3 Efficiency in establishing cell cultures, and culture lifespan

In 'Phase I' of this study, we aimed to employ our slightly modified Liu *et al*. (2016)

method to evaluate the efficiency of establishing keratinocyte cultures from biopsy specimens, and to assess their *in vitro* lifespan. The aim of this study was to determine whether we could establish cultures frequently enough and with a sufficient lifespan for further downstream experimentation (e.g. Western blot analysis, RNA extraction and qPCR, organotypic raft cultures, etc.). Interestingly, our results were nearly identical to Schweinfurth *et al*. (2006) who reported an efficiency of ~32% (n=7 of 22 biopsies) compared to our ~32% (n=8 of 25), and reported an average lifespan of 30 days in culture, compared to our 4 weeks. Additionally, their longest culture lasted 60 days, whereas ours grew for 8 weeks. Despite this similarity, it is important to note that these metrics do not truly reflect the overall population doublings in either case, and this result is only comparable if the doubling time is similar between our cultures and those of Schweinfurth *et al*. (2006) – which they did not report. Schweinfurth *et al*. (2006) also acquired their specimens from the oropharynx and established their cultures in NIKS medium, rather than a serum-free keratinocyte growth media. Therefore, it is difficult to confidently make comparisons between these different experimental conditions. For our 'Phase I' study however, it is important to note that larger biopsy specimens had a greater probability of establishing a culture, which added a predictive factor to our methods.

When establishing normal cervical keratinocyte cultures from hysterectomies, Liu *et al*. (2013) reported a maximum *in vitro* lifespan of approximately 6 weeks: 2 weeks to establish cultures in T-25 flasks, and one week between passages. Importantly, subsequent passages were seeded at a 1:2 ratio from the previous passage, indicating a long doubling time. Similar results were achieved when culturing keratinocytes from CIN biopsy specimens, wherein cultures could again be passaged 1:2 up to four times (Liu *et al*., 2016).

Our 'Phase I' results seem comparable with this, but somewhat more variable: of 7 proliferating cultures, 2 differentiated in the first T-12.5 flask, 3 differentiated in the first scale-up to a T-25, and 2 managed to be scaled up to a T-75 and passaged onto a second T-75. These results could be accounted for by biopsy size between research groups, slight methodological differences, or perhaps simply due to our larger sample size.

Though we felt our methodology was firmly established and our results reflected that of literature, we sought to improve culture conditions with the aim of increasing *in vitro* lifespan. We changed our culture media to EpiLife supplemented with HKGS, as this commercial media is rated for over twice as many population doublings versus conventional keratinocyte growth media (Li S *et al*., Cascade Biologics Inc). In addition, we added the ROCK inhibitor Y-27632, as this chemical inhibitor increases the *in vitro* lifespan of epithelial cells. In our method, the ROCK inhibitor was added after cultures were established in the presence of 5% FBS. This is because Y-27632 increases the growth rate of primary fibroblasts (Piltti *et al.*, 2015), and could potentially increase fibroblast contamination when establishing keratinocyte colonies from the processed biopsy specimens. In the presence of J2 feeders, ROCK inhibition is also capable of immortalizing primary epithelial cells, and has been employed for generating primary breast and prostate cell lines (Gil *et al*., 2005), as well as keratinocytes (Chapman *et al.*, 2011). For normal keratinocytes, ROCK inhibition alone increases total population doublings *in vitro* (Strudwick*et al*., 2015), and when combined with constitutive Myc or E6 expression, ROCK inhibition can immortalize keratinocytes. Although it is not fully understood, ROCK inhibition facilitates immortalization by reducing apoptosis and differentiation, in part by decreasing the expression of p53 target genes (Dakic *et al*., 2016). Therefore, we

hypothesized that ROCK inhibition should not only increase culture lifespan, but it may permit the immortalization of HPV-infected keratinocytes – as long as they continue to stably express E6. Despite this rationale, we did not obtain any immortalized cultures via this method. Additionally, keratinocyte subcultures recovered from cryopreserved stocks survived for just as many population doublings as their unpreserved counterparts (data not shown), suggesting that *in vitro* lifespan may be predetermined under these culture conditions. Interestingly, while the median lifespan, in weeks, remains largely unchanged, the switch to EpiLife containing Y-27632 drastically reduced the doubling time of keratinocytes, by roughly one half. Therefore, a subset of our established cultures proliferated for enough time – and with sufficient flask size-scaling – to yield ample cell numbers for downstream experimentation. Indeed, two cultures, AV6 and 3UI, reached passage numbers similar to that of commercially acquired keratinocytes. Interestingly, the patient information we acquired – age, lesion grade, and HPV type(s) – offered no real predictive value in establishing a proliferating culture. The biopsy size, and whether the biopsy was susceptible to collagenase digestion (i.e. yielding a turbid digest) were the most notable predictors of establishing cultures.

Although it was not tested in this study, future experiments should attempt to utilize J2 feeder layers in combination with Y-27632 to immortalize patient-derived keratinocyte cultures. The most prominent hurdle in utilizing feeders is the significant potential for fibroblast contamination. In this study, serum-free conditions drastically reduced the proliferation of residual fibroblasts; however, they were still visibly present in freshly established keratinocyte cultures. It was also evident that EpiLife increased fibroblast growth as compared to KGM, as it is a richer medium. We anticipate that residual

fibroblasts likely exist as a small percentage of the culture population for at least the first few passages. In two patient cultures, it was noted that the reintroduction of serum to less than 0.01% in an EpiLife background resulted in a rapid regrowth of fibroblasts (**Figure A10**). As standard feeder layers require serum, impure keratinocyte cultures remain the most prominent hurdle for immortalizing keratinocytes with feeders. It may be possible to serially dilute keratinocytes onto feeder layers to phase out their presence, or alternatively, cultures may need to be passaged several times before feeder layers can be introduced. Ideally, feeder layers and Y-27632 would be introduced as early as possible to ensure the long-term retention of patient cultures, and avoid the loss of otherwise successfully established cultures that possess too short a lifespan for experimental purposes.

4.4 Organotypic raft culturing

In this study, we were unable to fully develop a raft protocol for these patient derived cell lines. In most instances, it appeared that the cultures had met their *in vitro* lifespan, as indicated by cell sizes and subsequent differentiation. Use of feeder-layers with Y-27632 may address this issue by conditionally immortalizing cells. Despite using the long-lived isolates for further method development, we were unable to achieve stratification. This result is in stark contrast to other cell lines and medias, where we have successfully grown raft cultures using primary human foreskin keratinocytes, NIKS immortalized keratinocytes (Jackson *et al.*, 2014), and gingival keratinocytes – all of which where grown in different culture media prior to raft construction (data not shown).

It is interesting to note that there appeared to be invasion on patient culture IW9. This patient was shown to have an HPV16 positive, CINII-III lesion and is the highest

grade lesion we were able to establish a culture from in the second phase, and margins that resembled invasion were evident in all technical replicates.

4.5 Future work

Future work should test different media formulations for raft cultures. Biomarkers relating to differentiation (eg. K5, K10, K14), as well as clinical markers relating to lesion grade (eg. p16^{INK4a}, TOPO2a, MCM2) should be assessed, which may be corroborated both in the patient's histology, and in the patient-derived raft *in vitro*. Eventually, patient-derived raft cultures could be used to test novel therapeutics. Lechanteur *et al*. (2017) utilized lipid nanoparticles containing E7-targeting siRNA to treat raft cultures *in vitro*. Working with immortalized cell lines, Lechanteur *et al*., (2017) performed IHC on raft sections to stain for cell-cycle and apoptosis markers. In future work – with established methods for generating patient-derived raft cultures – it may be possible to test E6-targeting DsiRNA on patient-specific rafts, as a novel approach towards personalized medicine.

5. References

Allen-Hoffmann BL, Schlosser SJ, Ivarie CA, Sattler CA, Meisner LF, O'Connor SL. 2000. Normal growth and differentiation in a spontaneously immortalized near-diploid human keratinocyte cell line, NIKS. *J Invest Dermatol* 114:444-455.

Banton RA, Perez-Reyes N, Merrick DT, McDougall JK. 1991. Epithelial cells immortalized by human papillomaviruses have premalignant characteristics in organotypic culture.

Bell E, Ehrlich HP, Buttle DJ, Nakatsuji T. 1981. Living tissue formed *in vitro* and accepted

as skin-equivalent tissue of full thickness. *Science* 211(4486):1052-1054.

Bentley J, EXECUTIVE COUNCIL OF THE SOCIETY OF CANADIAN COLPOSCOPISTS, SPECIAL CONTRIBUTORS. 2012. Colposcopic management of abnormal cervical cytology and histology. *J Obstet Gynaecol Can* 34(12):1188-1202.

Birmingham A, Anderson E, Reynolds A, Ilsley-Tyree D, Leake D, Federov Y, Baskerville S, Maksimova E, Robinson K, Karpilow J, Marshall WS, Khvorova A. 2006. 3' UTR seed matches, but not overall identity, are associated with RNAi off-targets. *Nature Methods* 3(3):199-204.

Bolard J, Joly V, Yeni P. 1993. Mechanism of action of amphotericin b at the cellular level, its modulation by delivery system. *J Liposom Res* 3(3):409-427.

Bononi I, Bosi S, Bonaccorsi G, Marci R, Patella A, Ferretti S, Tognon M, Garutti P, Martini F. 2012. Establishment of keratinocyte colonies from small-sized cervical intraepithelial neoplasia specimens. *J Cell Physio* 227:3787-3795.

Buehler E, Chen YC, Martin S. 2012. C911: A bench-level control for sequence specific siRNA off-target effects. *PLOS One* 7(12):e51942.

Bustin SA, Benes V, Garson JA, Hellemans J, Huggett J, Kubista M, Mueller R, Nolan T, Pfaffl MW, Shipley GL, Vandesompele J, Wittwer CT. The MIQE guidelines: minimum information for publication of quantitative real-time PCR experiments. *Clin Chem* 55(4):611-622.

Cattani P, Zannoni GF, Ricci C, D'Onghia S, Trivellizzi IN, Di Franco A, Vellone VG, Durante M, Fadda G, Scambia G, Capelli G, De Vincenzo R. 2009. Clinical performance of human papillomavirus E6 and E7 mRNA testing for high-grade

lesions of the cervix. *J Clin Microbiol* 47(12):3895–3901.

Chapman S, Liu X, Meyers C, Schlegel R, McBride AA. 2011. Human keratinocytes are efficiently immortalized by a Rho kinase inhibitor. *J Clin Invest* 120:2619–2626.

Crow JM. 2012. HPV: the global burden. *Nature* 488(7418):S2-S3.

Dakic A, DiVito K, Fang S, Suprynowicz F, Gaur Anirudh, Li X, Palechor-Ceron N, Simic V, Choudhury S, Yu S, Simbulan-Rosenthal CM, Rosenthal D, Schlegel R, Liu X. 2016. ROCK inhibitor reduces Myc-induced apoptosis and mediates immortalization of human keratinocytes. *Oncotarget* 7(41):66740-66753.

Dawson CW, Dawson J, Jones R, Ward K, Young LS. 1998. Functional differences between BHRF1, the Epstein-Barr virus-encoded Bcl-2 homologue, and Bcl-2 in human epithelial cells. *J Virol* 72(11):9016-9024.

DeCarlo CA, Escott NG, Werner J, Robinson K, Lambert PF, Law RD, Zehbe I. 2008. Gene expression analysis of interferon kappa in laser capture microdissected cervical epithelium. *Anal Biochem* 381:59-66.

de Villiers EM. 2013. Cross-roads in the classification of papillomavirus. *Virology* 455(1-2):2-10.

Dongari-Bagtzoglou A, Kashleva H. 2006. Development of a highly reproducible three-dimensional organotypic model of the oral mucosa. *Nat Protoc* 1(4):2012-2018.

Duraffour S, Snoeck R, de Vos R, van Den Oord JJ, Crance JM, Garin D, Hruby DE, Jordan R. 2007. Activity of the anti-orthopoxvirus compound ST-246 against vaccinia, cowpox and camelpox viruses in cell monolayers and organotypic raft cultures. *Antivir Ther* 12:1205-1216.

Eicher SA, Clayman GL, Liu TJ, Shillitoe EJ, Storthz KA, Roth JA, Lotan R. Evaluation

of topical gene therapy for head and neck squamous cell carcinoma in an organotypic model. *Clin Cancer Res* 2:1659-1664.

Fadok VA, Voelker DR, Campbell PA, Cohen JJ, Bratton DL, Henson PM. 1992. Exposure of phosphatidylserine on the surface of apoptotic lymphocytes triggers specific recognition and removal by macrophages. *J Immunol* 148(7):2207-2216.

Fire A, Xu S, Montgomery MK, Kostas SA, Driver SE, Mello CC. 1998. Potent and specific genetic interference by double-stranded RNA in *Caenorhabtidis elegans*. *Nature* 391:806-811.

Fischer AB. 1975. Gentamicin as a bactericidal antibiotic in tissue culture. *Med Microbiol Immunol* 161:23-39.

Flores ER, Allen-Hoffmann BL, Lee D, Sattler CA, Lambert PF. 1999. Establishment of the human papillomavirus type 16 (HPV-16) life cycle in an immortalized human foreskin keratinocyte cell line. *Virology* 262:344-354.

Frattini MG, Laimins LA. 1994. Binding of the human papillomavirus E1 origin-recognition protein is regulated through complex formation with the E2 enhancer-binding protein. *Proc Natl Acad Sci* 91:12398 – 12402.

Friedl F, Kimura I, Osato T, Ito Y. 1970. Studies on a new human cell line (SiHa) derived from carcinoma of uterus. I. Its establishment and morphology. *Proc Soc Exp Biol Med* 135(2):543-545.

Genther SM, Sterling S, Duensing S, Munger K, Sattler C, Lambert PF. 2003. Quantitative role of the human papillomavirus type 16 E5 gene during the productive stage of the viral life cycle. *J Virol* 77:2832–42.

Gil J, Kerai P, Lleonart M, Bernard D, Cigudosa JC, Peters G, Carnero A, Beach D. 2005.

Immortalization of primary human prostate epithelial cells by c-Myc. *Cancer Res* 65:2179–2185.

Gonzalez DI, Zahn CM, Retzloff MG, Moore WF, Kost ER, Snyder RR. 2001. Recurrence of dysplasia after loop electrosurgical excision procedures with long-term follow-up. *Am J Obstet Gynecol* 184(3):315-21.

Halloush RA, Akpolat I, Jim Zhai Q, Schwartz MR, Mody DR. 2008. Comparison of ProEx C with p16INK4a and Ki-67 immunohistochemical staining of cell blocks prepared from residual liquid-based cervicovaginal material: a pilot study. *Cancer* 114(6):474–480.

Hammond SM, Bernstein E, Beach D, Hannon GJ. 2000. An RNA-directed nuclease mediates post-transcriptional gene silencing in *Drosophila* cells. *Nature* 404(6775):293-296.

Hanning JE, Saini HK, Murray MJ, van Dongen S, Davis MPA, Barker EM, Ward DM, Scarpini CG, Enright AJ, Pett MR, Coleman N. 2013. Lack of correlation between predicted and actual off-target effects of short-interfering RNAs targeting the human papillomavirus type 16 E7 oncogene. *Br J Cancer* 108(2):450-460.

Ho GY, Bierman R, Beardsley L, Chang CJ, Burk RD. 1998. Natural history of cervicovaginal papillomavirus infection in young women. *N Engl J Med* 338(7):423-428.

Hukkanen V, Mikola H, Nykanen M, Syrjanen S. 1999. Herpes simplex virus type 1 infection has two separate modes of spread in three-dimensional keratinocyte culture. *J Gen Virol* 80:2149-2155.

Jackson AL, Bartz SR, Schelter J, Kobayashi SV, Burchard J, Mao M, Li B, Cavet G,

Linsley PS. 2003. Expression profiling reveals off-target gene regulation by RNAi. *Nat Biotechnol* 21(6):635-637.

Jackson AL, Burchard J, Schelter J, Chau BN, Cleary M, Lim L, Linsley PS. 2006. Widespread siRNA "off-target" transcript silencing mediated by seed region sequence complementarity. *RNA* 12(7):1179-1187.

Jackson R, Togtema M, Lambert PF, Zehbe I. 2014. Tumourigenesis driven by the human papillomavirus type 16 Asian-American e6 variant in a three-dimensional keratinocyte model. *PLOS One* 9(7):e101540.

Jiang M, Milner J. 2002. Selective silencing of viral gene expression in HPV-positive human cervical carcinoma cells treated with siRNA, a primer of RNA interference. *Oncogene* 21:6041-6048.

Kajitani N, Satsuka A, Kawate A, Sakai H. 2012. Productive lifecycle of human papillomaviruses that depends upon epithelial differentiation. *Front Microbiol* 3(152):1-12.

Khairuddin N, Blake SJ, Firdaus F, Steptoe RJ, Behlke MA, Hertzog PJ, McMillan NA. 2014. In vivo comparison of local versus systemic delivery of immunostimulating siRNA in HPV-driven tumours. *Immunol Cell Biol* 92(2):156-163.

Kim DH, Behlke MA, Rose SD, Chang MS, Choi S, Rossi JJ. 2005. Synthetic dsRNA Dicer substrates enhance RNAi potency and efficacy. *Nat Biotechnol* 23(2):222–226.

Klingelhutz AJ, Roman Ann. 2012. Cellular transformation by human papillomaviruses: lessons learned by comparing high- and low-risk viruses. *Virology* 424(2):77-98.

Koopman G, Reutelingsperger CP, Kuijten GA, Keehnen RM, Pals ST, van Oers MH.

1994. Annexin V for flow cytometric detection of phosphatidylserine expression on B cells undergoing apoptosis. *Blood* 84(5):1415-1420.

Lechanteur A, Furst T, Evrard B, Delvenne P, Piel G, Hubert P. 2017. Promoting vaginal distribution of E7 and MCL-1 siRNA-silencing nanoparticles for cervical cancer treatment. *Mol Pharm* 14(5):1706-1717.

Leitz J, Reuschenbach M, Lohrey C, Honegger A, Accardi R, Tommasino M, Llano M, von Knebel Doeberitz M, Hoppe-Seyler K, Hoppe-Seyler F. 2014. Oncogenic human papillomaviruses activate the tumor-associated lens epithelial-derived growth factor (LEDGF) gene. *PLOS Pathog* 10(3):e1003957.

Li S, Donahue LM, Shipley AK, Droms KA, Lin Y, Cook PW, Shipley GD. Altering basal medium components increases the *in vitro* lifespan of normal human keratinocytes. Cascade Biologics Inc, Portland Oregon (Poster).

Liu Y, Lu X, Pan Z, Zhang W, Chen Z, Wang H, Liu H, Zhang Y. 2013. Establishment of a novel method for primary culture of normal human cervical keratinocytes. *Chin Med J* 126(17):3344-3347.

Liu Y, Wang T, Zhang Y. 2016. A modified method for the culture of naturally HPV-infected high-grade cervical intraepithelial neoplasia keratinocytes from human neoplastic cervical biopsies. *Oncol Lett* 11:1457-1462.

Livak KJ, Schmittgen TD. 2001. Analysis of relative gene expression data using real-time quantitative PCR and the $2^{(-\Delta\Delta c(t))}$ method. *Methods* 25(4):402-408.

McGarrity GJ, Barile MF. 1983. Use of indicator cell lines for recovery and identification of cell culture mycoplasmas. *In* Tully J (ed), Methods in mycoplasmology V2: diagnostic mycoplasmology, Academic Press, New York p. 167-170.

McLaughlin-Drubin ME, Meyers J, Munger K. 2012. Cancer associated human papillomaviruses. *Curr. Opin Virol*. 2(4):459-466.

Meyers C, Frattini MG, Hudson JB, Laimins LA. 1992. Biosynthesis of human papillomavirus from a continuous cell line upon epithelial differentiation. *Science* 257:971-973.

Moll R, Franke WW, Schiller DL, Geiger B, Krepler R. 1982. The catalog of human cytokeratins: patterns of expression in normal epithelia, tumors and cultured cells. *Cell* 31:11–24.

Mosmann T. 1983. Rapid colorimetric assay for cellular growth and survival: application to proliferation and cytotoxicity assays. *J Immunol Methods* 65:55-63.

Neely EK, Morhenn VB, Hintz RL, Wilson DM, Rosefield RG. 1991. Insulin-like growth factors are mitogenic for human keratinocytes and squamous cell carcinoma. *J Invest Dermatol* 96(1):104-110.

Nykanen A, Haley B, Zamore PD. 2001. ATP requirements and small interfering RNA: structure in the RNA interference pathway. *Cell* 107:309-321.

Pattillo RA, Hussa RO, Story MT, Ruckert AC, Shalaby MR, Mattingly RF. 1977. Tumor antigen and human chorionic gonadotropin in CaSki cells: a new epidermoid cervical cancer cell line. *Science* 196(4297):1456-1458.

Peh WL, Brandsma JL, Christensen ND, Cladel NM, Wu X, Doorbar J. 2004. The viral E4 protein is required for the completion of the cottontail rabbit papillomavirus (CRPV) productive cycle in vivo. *J Virol* 15:2142–51.

Peitsaro P, Johansson B, Syrjanen S. 2002. Integrated human papillomavirus type 16 is frequently found in cervical cancer precursors as demonstrated by a novel

quantitative real-time PCR technique. *J Clin Microbiol* 40:886-891.

Persengiev SP, Zhu X, Green MR. 2004. Nonspecific, concentration-dependent stimulation and repression of mammalian gene expression by small interfering RNAs (siRNAs). *RNA* 10(1):12-8.

Pickard A, McDade SS, McFarland M, McCluggage WG, Wheeler CM, McCance DJ. 2015. HPV16 down-regulates the insulin-like growth factor binding protein 2 to promote epithelial invasion in organotypic cultures. *PLOS Pathog* 11(6):e1004988.

Piltti J, Varjosalo M, Qu C, Hayrinen J, Lammi MJ. 2015. Rho-kinase inhibitor Y-27632 increases cellular proliferation and migration in human foreskin fibroblast cells. *Proteomics* 15:2953-2965.

R Core Team. 2013. R: a language and environment for statistical computing. R Foundation for Statistical Computing.

R Studio Team. 2015. RStudio: integrated development for R. RStudio, Inc., Boston, MA.

Schweinfurth JM, Meyers C. 2006. Organotypic (raft) culture of biopsy-derived upper respiratory epithelium. *Laryngoscope* 116:1600-1602.

Rheinwald JG, Beckett MA. 1981. Tumorigenic keratinocyte lines requiring anchorage and fibroblast support cultured from human squamous cell carcinomas. *Cancer Res* 41:1657-1663.

Sasaoka T, Ishiki M, Sawa T, Ishihara H, Takata Y, Imamura T, Usui I, Olefsky JM, Kobayashi M. 1996. Comparison of the insulin and insulin-like growth factor 1 mitogenic intracellular signalling pathways. *Endocrinology* 137(10):4427-4434.

Shapiro HM. 1988. Practical Flow Cytometry, second edition. p.353 Alan R. Liss, Inc, New York.

Smotkin D, Prokoph H, Wettstein FO. 1989. Oncogenic and nononcogenic human genital papillomaviruses generate the E7 mRNA by different mechanisms. *J Virol* 63:1441-1447.

Stanley MA. 2002. Culture of human cervical epithelial cells, p137-169. *In* Freshney RI, Freshney MG (ed), Culture of epithelial cells, 2nd ed, Wiley-Liss, New York.

Strudwick XL, Lang DL, Smith LE, Cowin AJ. 2015. Combination of low calcium with Y-27632 ROCK inhibitor increases the proliferative capacity, expansion potential and lifespan of primary human keratinocytes while retaining their capacity to differentiate into stratified epidermis in a 3D skin model. *PLOS One* 10(4):e0123651.

Tait JF, Gibson D. 1992. Phospholipid binding of annexin V: effects of calcium and membrane phosphatidylserine content. *Arch Biochem Biophys* 298(1):187-191.

Taylor-Robinson D, Bebear C. 1997. Antibiotic susceptibilies of mycoplasmas and treatment of mycroplasma infections. *J Antimicrob Chemother* 40:662-630.

Togtema M, Jackson R, Grochowski J, Villa PL, Mellerup M, Chattopadhyaya J, Zehbe I. Synthetic siRNA targeting human papillomavirus 16 E6: a perspective on *in vitro* nanotherapeutic approaches. *Nanomedicine* (in press).

Waterhouse PM, Graham MW, Wang MB. 1998. Virus resistance and gene silencing in plants can be induced by simultaneous expression of sense and antisense RNA. *Proc Natl Acad Sci* 95:13959–13964 .

Wentzensen N, von Knebel Doeberitz M. 2007. Biomarkers in cervical cancer. *Dis Markers* 23(4):315-330.

Wilson VG, West M, Woytek K, Rangasamy D. 2002. Papillomavirus E1 proteins: form,

function, and features. *Virus Genes* 24:275–90.

Woodman CBJ, Collins SI, Young LS. 2007. The natural history of cervical HPV infections: unresolved issues. *Nature Rev Cancer* 7(1):11-22.

Zheng ZM, Baker CC. 2006. Papillomavirus genome structure, expression, and post-transcriptional regulation. *Front Biosi* 11:2286-2302.

Zubach V, Smart G, Ratnam S, Severini A. 2012. A novel microscphere-based method for the detection and typing of 46 mucosal human papillomavirus types. *J Clin Microbiol* 50(2):460-464.

zur Hausen H. 2002. Papillomavirus and cancer: from basic studies to clinical application. *Nature Rev Cancer* 2:342-350.

Appendix

Statistics (9)	Events	% of Vis	X Mean	Y Mean	X GeoMean	Y GeoMean	X Median	Y Median
All events	9,926	100.00	21.33	25.95	9.09	4.98	7.77	3.43
Left Bottom	8,211	82.72	7.93	4.04	6.72	3.10	6.79	2.86
Right Bottom	644	6.49	52.56	11.69	37.69	8.96	30.51	11.65
Left Top	366	3.69	9.68	181.50	8.15	115.55	8.74	100.90
Right Top	705	7.10	154.99	213.35	88.52	138.96	69.16	191.10
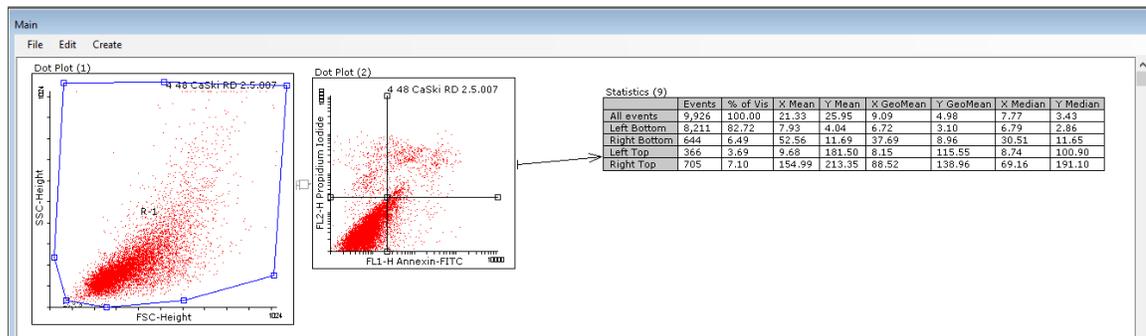
Figure A1. Screenshot of dot plot following Annexin V-FITC and propidium iodide staining for apoptosis analysis. Data was analyzed in Flowing Software 2.0 and statistical summaries were exported and analyzed in R (performed by Robert Jackson).
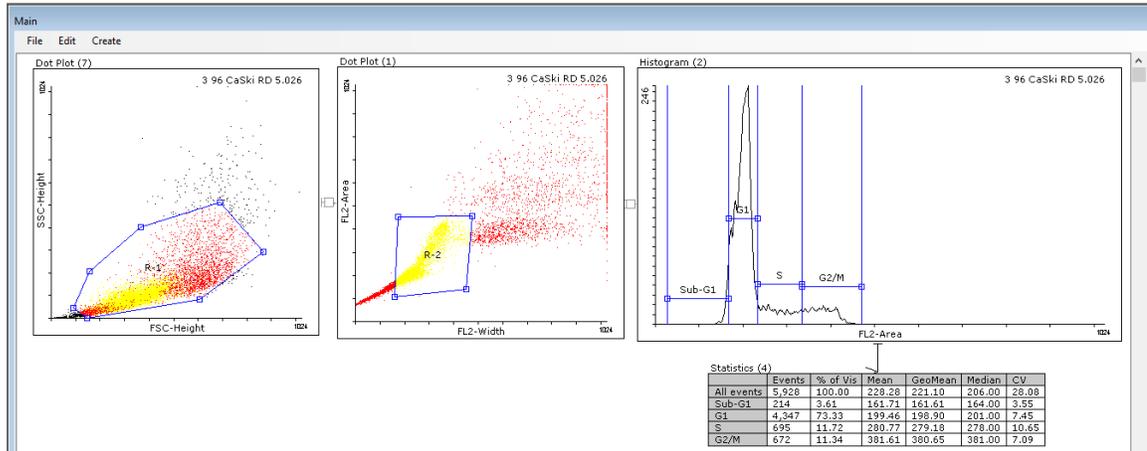
Figure A2. Screenshot of workflow and histogram used in cell-cycle analysis. Data was analyzed in Flowing Software 2.0 and statistical summaries were exported and analyzed in R (performed by Robert Jackson).
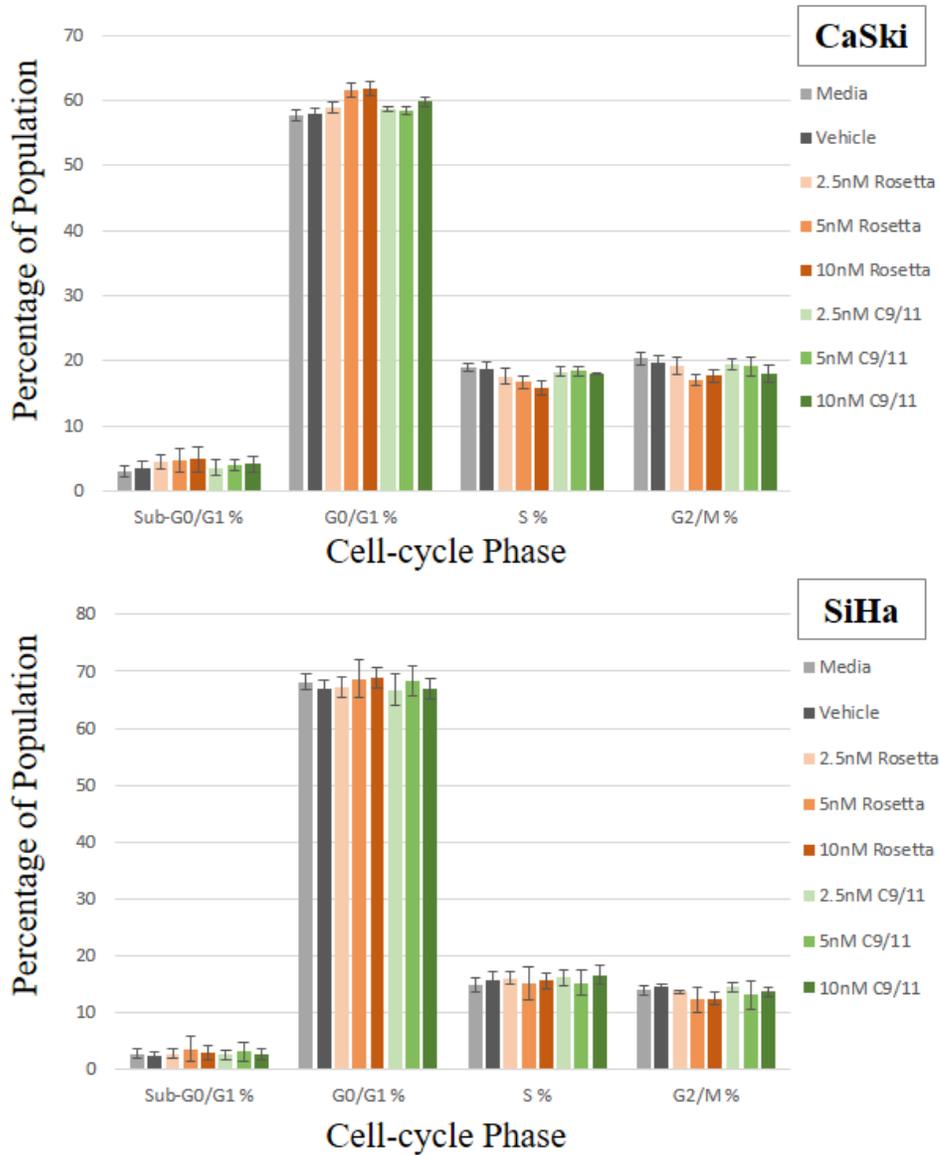
Figure A3. Cell-cycle analysis of CaSki and SiHa 48 hours after transfection. Cultures were transfected with Rosetta DsiRNA or C9/11 DsiRNA control and harvested 48 hours later. Cells were stained with propidium iodide for flow cytometric analysis of cell cycle. No significant differences in cell-cycle phases was found between Rosetta and C9/11 controls. Data represent mean ± SD (n=3).
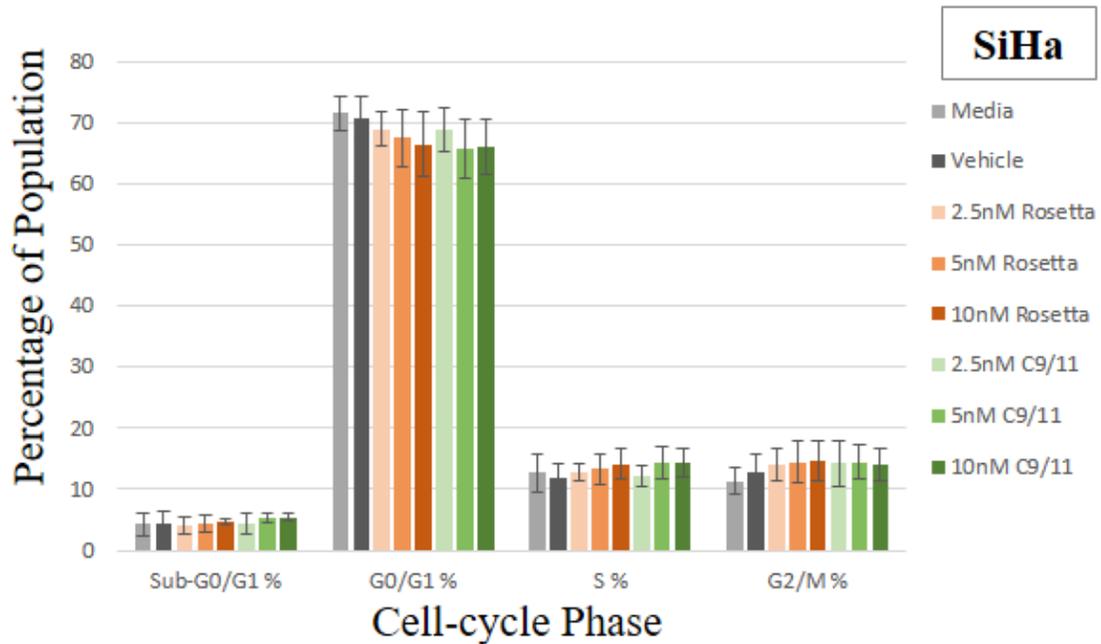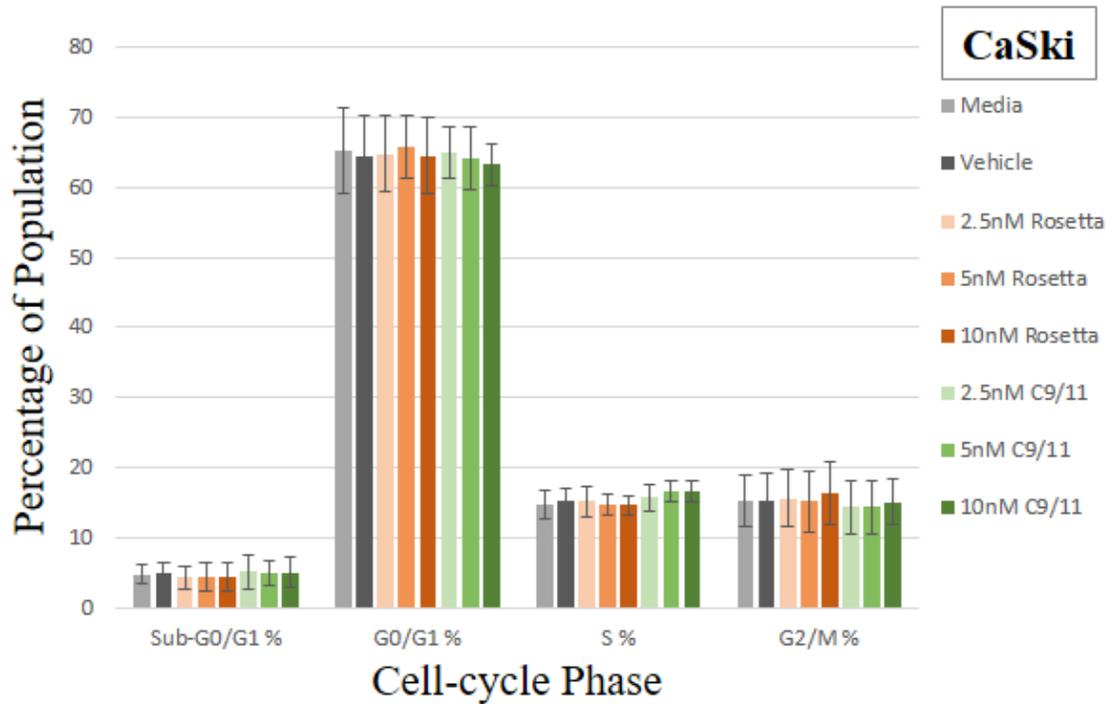
Figure A4. Cell-cycle analysis of CaSki and SiHa 96 hours after transfection. Cultures were transfected with Rosetta DsiRNA or C9/11 DsiRNA control and harvested 96 hours later. Cells were stained with propidium iodide for flow cytometric analysis of cell cycle. No significant differences in cell-cycle phases was found between Rosetta and C9/11 controls. Data represent mean ± SD (n=3).
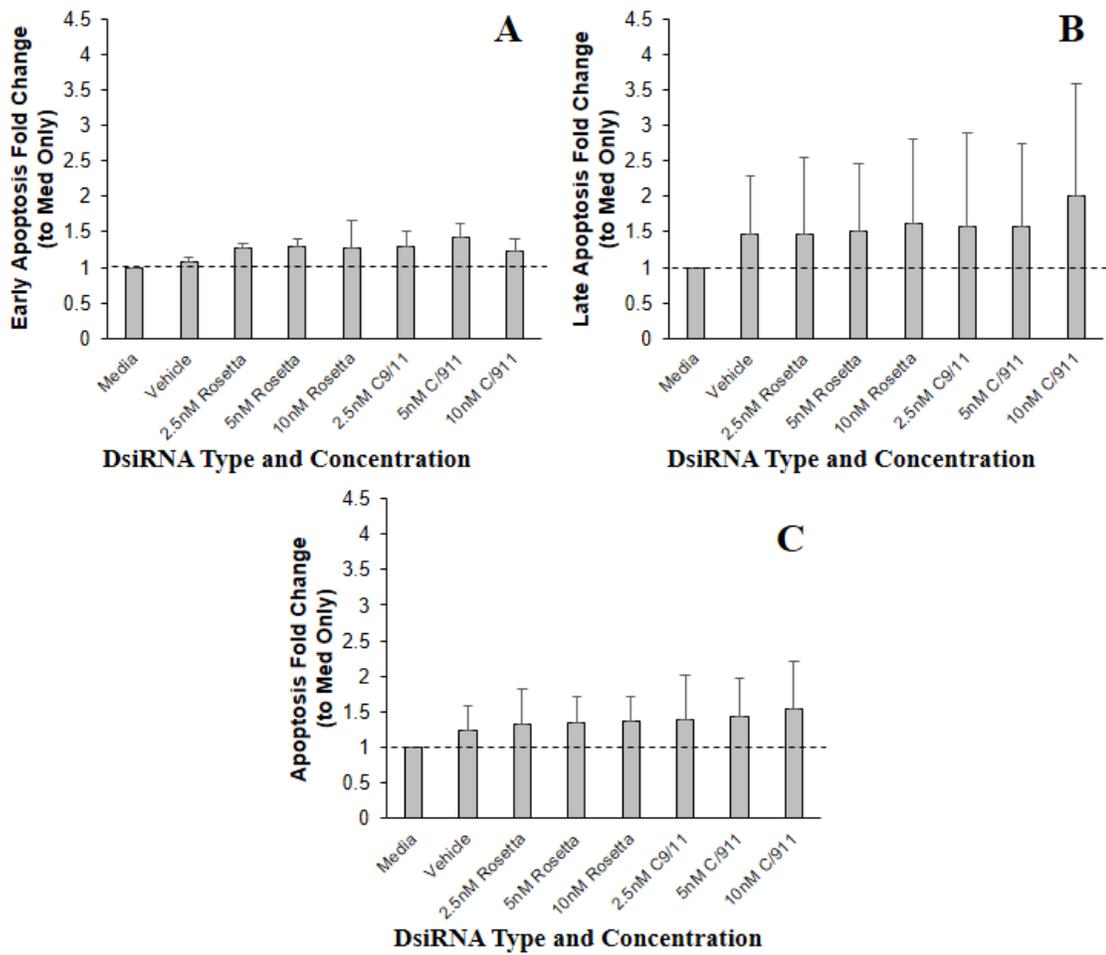
Figure A5. Flow cytometry analysis of apoptotic events in CaSki at 48 hours. Cultures were treated with Rosetta or C9/11 DsiRNA. Apoptosis was measured using Annexin V – FITC and propidium iodide. No statistical changes in apoptosis were found for early (**A**), late (**B**), or total (**C**). Data represent mean ± SD (n=3).
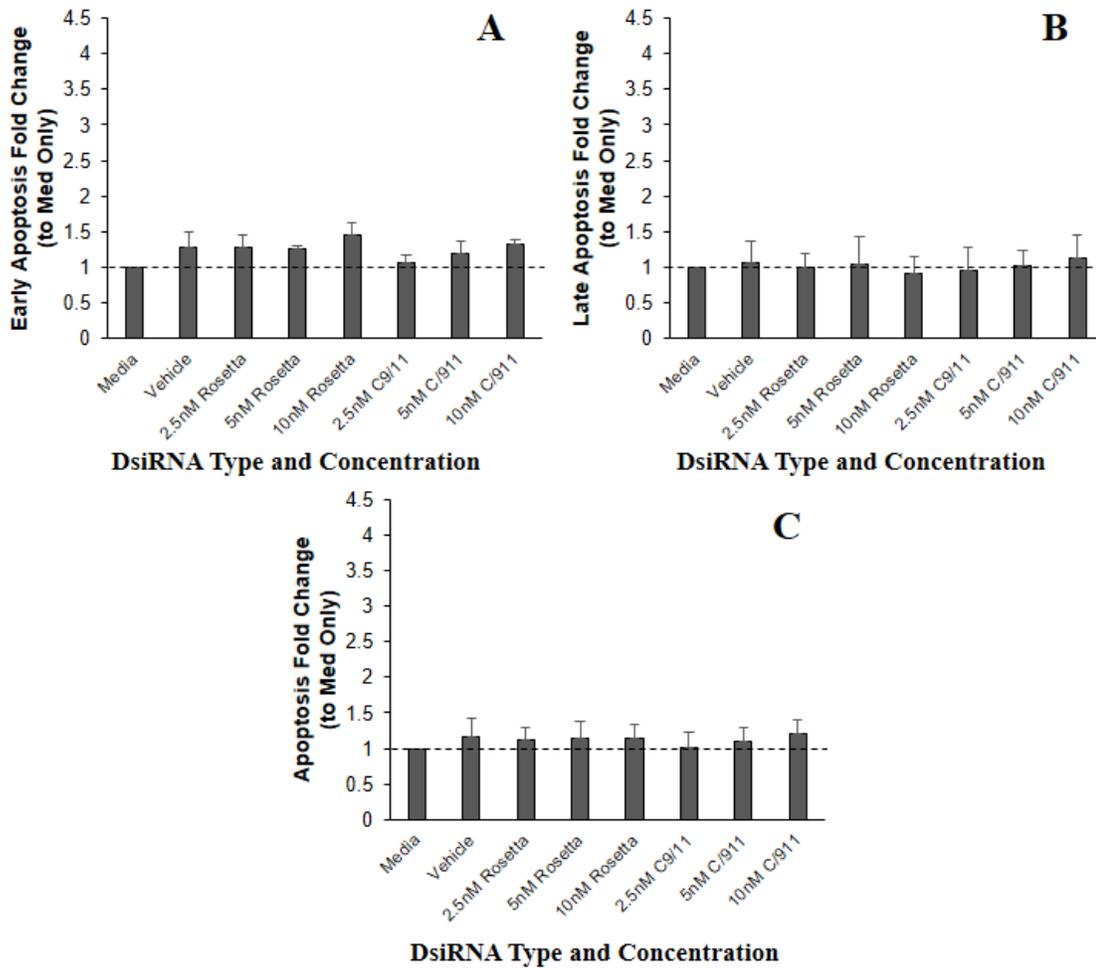
Figure A6. Flow cytometry analysis of apoptotic events in SiHa at 48 hours. Cultures were treated with Rosetta or C9/11 DsiRNA. Apoptosis was measured using Annexin V – FITC and propidium iodide. No statistical changes in apoptosis were found for early (**A**), late (**B**), or total (**C**). Data represent mean ± SD (n=3).
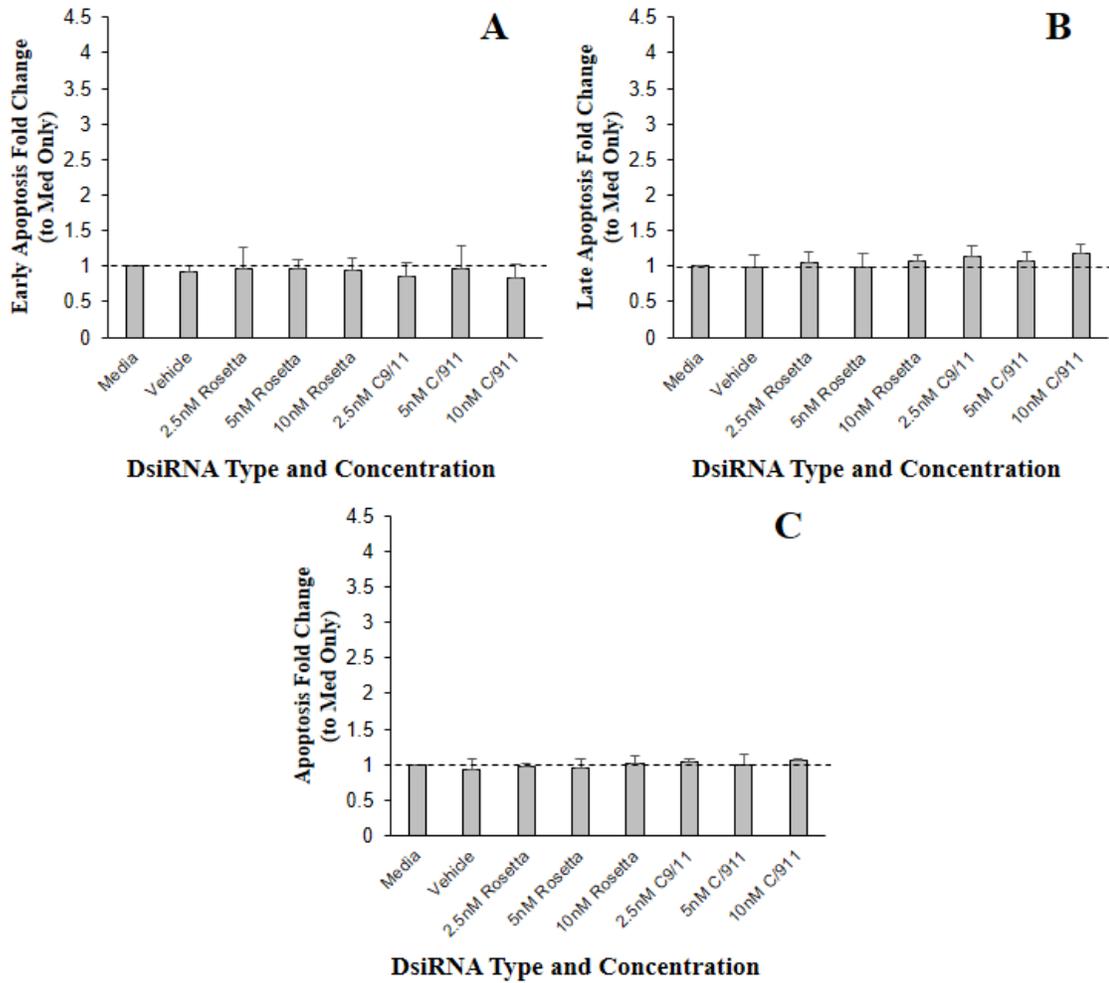
Figure A7. Flow cytometry analysis of apoptotic events in CaSki at 96 hours. Cultures were treated with Rosetta or C9/11 DsiRNA. Apoptosis was measured using Annexin V – FITC and propidium iodide. No statistical changes in apoptosis were found for early (**A**), late (**B**), or total (**C**). Data represent mean ± SD (n=3).
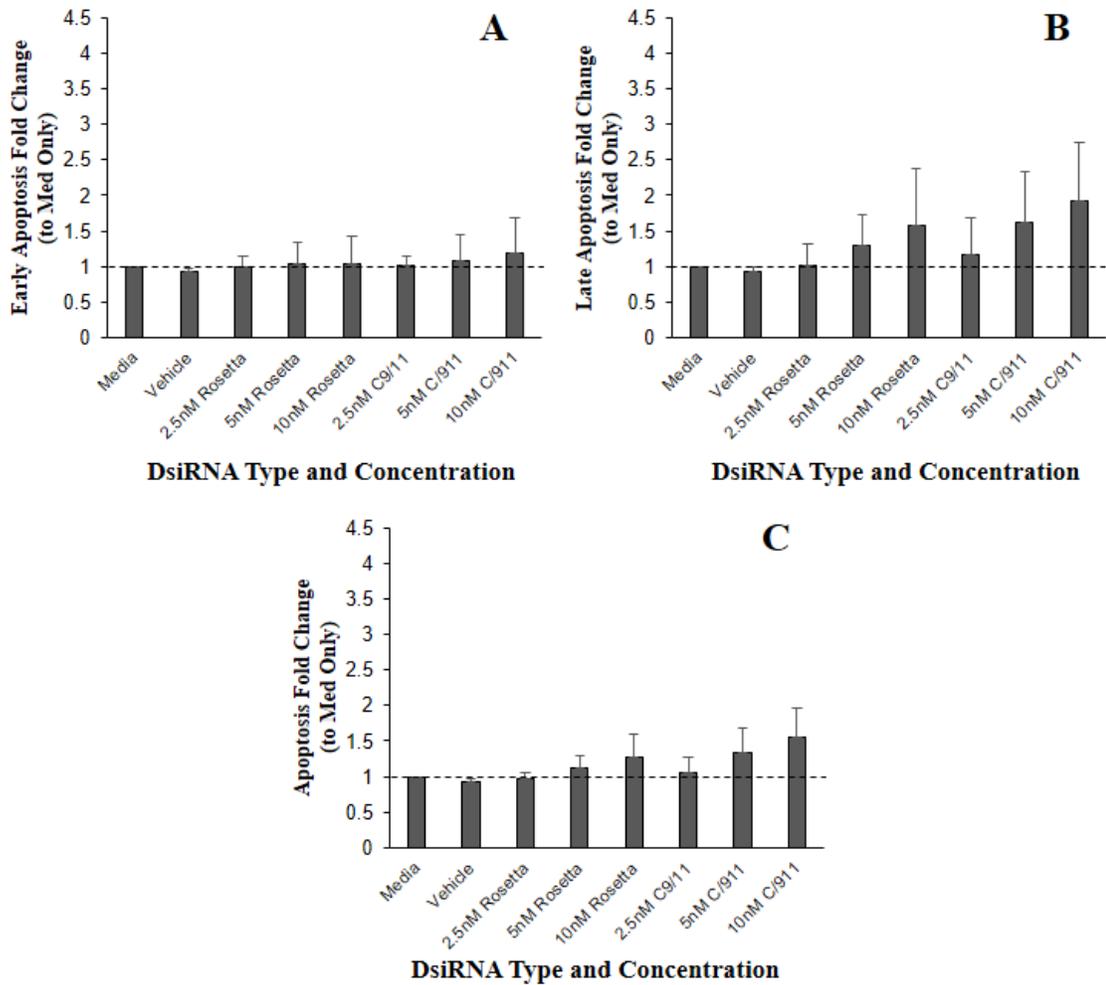
Figure A8. Flow cytometry analysis of apoptotic events in SiHa at 96 hours. Cultures were treated with Rosetta or C9/11 DsiRNA. Apoptosis was measured using Annexin V – FITC and propidium iodide. No statistical changes in apoptosis were found for early (**A**), late (**B**), or total (**C**). Data represent mean ± SD (n=3).
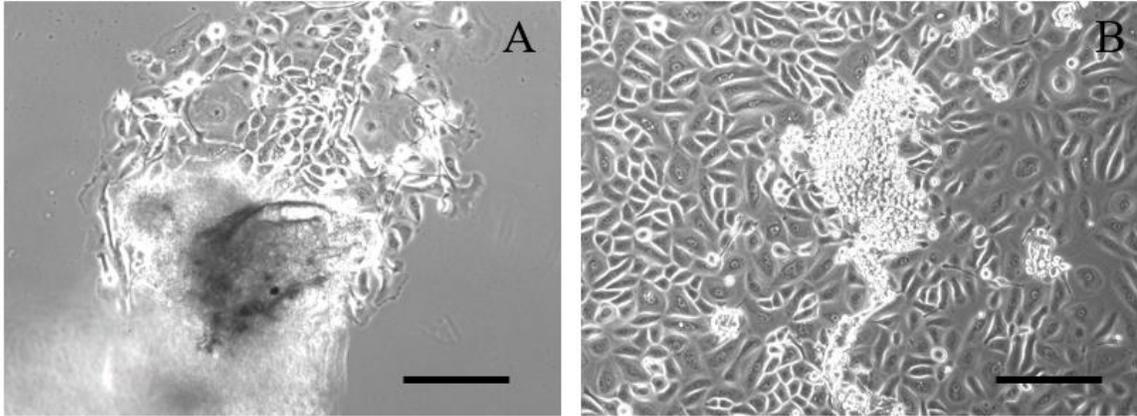
Figure A9. Keratinocyte colonies seeded by fragments of partially digested tissue. Partially digested tissue fragments seed colonies in some patients (**A** and **B**), behaving as pseudo-explant cultures. Scale bar represents 200 microns.
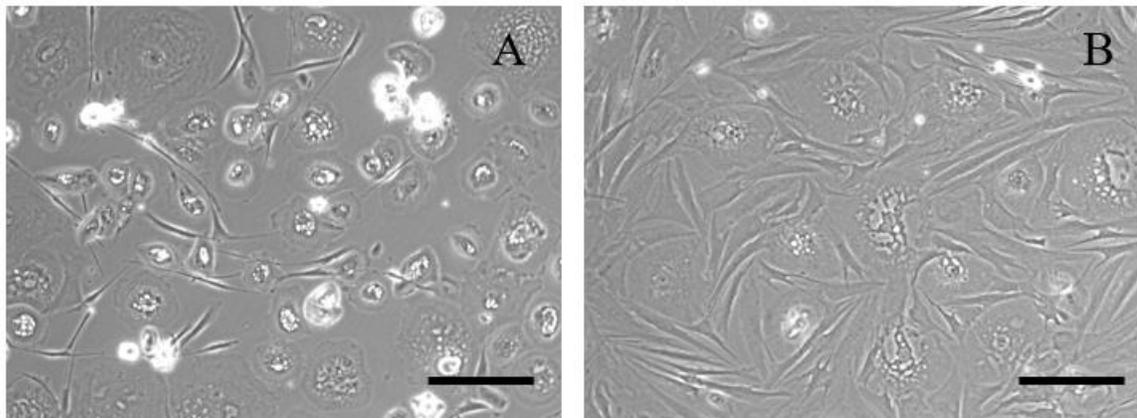

Figure A10. Fibroblast regrowth after the re-introduction of serum in the presence of EpiLife. Cultures were reseeded into EpiLife with Y-27632, from a 10 µl of cells suspended in NIKS medium, leftover from seeding raft cultures. At a final concentration of <0.01% FBS, fibroblasts regrew within a week. Colony of fibroblasts amongst differentiated keratinocytes from A1U (**A**) and fibroblast confluence in IW9 (**B**). Scale bar represents 200 microns.